



CM-P00060972

Submitted to
Nuclear Physics B

CERN/D.Ph.II/PHYS 74-17
(Ref. TH - 1800-CERN)
22.5.1974

Archives

RAPIDITY CORRELATIONS AT FIXED MULTIPLICITY IN

CLUSTER EMISSION MODELS

Edmond L. Berger

CERN, Geneva

ABSTRACT

Rapidity correlations in the central region among hadrons produced in proton-proton collisions of fixed final state multiplicity n at NAL and ISR energies are investigated in a two-step framework in which clusters of hadrons are emitted essentially independently, via a multiperipheral-like model, and decay isotropically. For $n \gtrsim \frac{1}{2} \langle n \rangle$, these semi-inclusive distributions are controlled by the reaction mechanism which dominates production in the central region. Thus, data offer cleaner insight into the properties of this mechanism than can be obtained from fully inclusive spectra. A method of experimental analysis is suggested to facilitate the extraction of new dynamical information. It is shown that the n dependence of the magnitude of semi-inclusive correlation functions reflects directly the structure of the internal cluster multiplicity distribution. This conclusion is independent of certain assumptions concerning the form of the single cluster density in rapidity space.

1. INTRODUCTION

The idea that hadrons are produced in clusters provides a popular interpretation [1,2] of several features of multiparticle production data at CERN Intersecting Storage Ring (ISR) and Fermi National Accelerator Laboratory (NAL) energies. In particular, the postulate of independent emission of isotropic clusters has been applied by several authors to reproduce the observed [3-7] positive, short range character of fully inclusive two-particle rapidity correlation functions in the central region. The general idea is that groupings of hadrons (clusters) are produced according to some basic dynamical amplitude, and that observed hadrons are decay products of these clusters. A crude sketch is given in fig. 1. At present, it is not clear that clusters have intrinsic dynamical significance (e.g. generalised resonances) or whether they are primarily a phenomenological artifice, a convenient imitation of more complex dynamics. Taking them seriously as dynamical entities, we should search for experimental quantities which would help to specify the character of the cluster production mechanism, as well as the intrinsic properties of clusters, such as their isospin, charge, spin, mass and multiplicity distributions.

Recently, data have become available on rapidity correlations in the central region at fixed values of the final state hadron multiplicity [8-10]. In this article I discuss in some detail what these semi-inclusive data may imply for clusters, in particular, for their intrinsic multiplicity distribution. Based on the concept of independent emission of isotropic clusters, expressions are derived and presented here for two particle semi-inclusive rapidity correlations in proton-proton collisions. A method of experimental analysis is suggested for extracting most directly the new physical content of semi-inclusive data. This article is an expanded, generalized version of a letter published earlier [11]. A number of phenomenological papers have appeared [12]; they may be consulted for other viewpoints.

Despite oft-stated reservations, I present the discussion in terms of the rapidity correlation function, as usually defined, but for fixed final state multiplicity n .

$$C_n(y_1, y_2) = \frac{1}{\sigma_n} \frac{d^2 \sigma_n}{dy_1 dy_2} - \left(\frac{1}{\sigma_n} \right)^2 \frac{d\sigma_n}{dy_1} \frac{d\sigma_n}{dy_2} . \quad (1.1a)$$

$$R_n(y_1, y_2) = C_n(y_1, y_2) / \left(\frac{1}{\sigma_n} \right)^2 \left(\frac{d\sigma_n}{dy_1} \right) \left(\frac{d\sigma_n}{dy_2} \right) . \quad (1.1b)$$

Variables associated with transverse momenta p_T are suppressed. In principle, it would be valuable to study y correlations for fixed \vec{p}_T . Thus, eq. (1.1) can be understood as applicable at each set of fixed \vec{p}_{T1} , or as expressions for quantities integrated over the p_T 's. Multiplicity index n may denote total charged multiplicity, pion multiplicity, negatives ..., etc. Cross section σ_n is the relevant partial cross section for multiplicity n . (All rapidities y are center of mass quantities).

The single and two-particle inclusive y spectra satisfy the normalization conditions

$$\frac{1}{\sigma_n} \int dy \frac{d\sigma_n}{dy} = n; \quad (1.2)$$

$$\frac{1}{\sigma_n} \iint dy_1 dy_2 \frac{d^2 \sigma_n}{dy_1 dy_2} = n(n-1); \quad (1.3)$$

and

$$\iint dy_1 dy_2 C_n(y_1, y_2) = -n \quad (1.4)$$

In eq. (1.3) the assumption is made that the two observed hadrons are identical; i.e. both are charged pions, both negatives, etc.

Semi-inclusive correlations provide several advantages and yield important information [11]. First, contributions to the correlation function from competing reaction types are more readily separated, removing a source of ambiguity which plagues analyses of the fully inclusive correlations. As discussed in sect. 3.2, by restricting multiplicity n to values $n \gtrsim \frac{1}{2} \langle n \rangle$, one should effectively eliminate diffractive contributions to $C_n(0,0)$. Semi-inclusive data at the larger n values reveal more cleanly properties of the reaction mechanism which dominates production in the central region.

Second, the postulate of isotropic cluster decay can be tested over a range of multiplicities. According to the models discussed here, the effective correlation length (δ) should be independent of n for $n \gtrsim \frac{1}{2} \langle n \rangle$.

Third, and perhaps most interesting, dependence of the intrinsic multiplicity distribution within clusters on the overall final state hadronic multiplicity can be investigated. A mean of $\langle k \rangle = 3$ to 4 total hadrons per cluster is determined from data on fully inclusive correlation functions [1]. However, this figure results after an average over both the multiplicity distribution of hadrons within clusters and the multiplicity distribution for production of clusters. Separation of the two effects is aided by fixing the final state hadronic multiplicity.

Defining $p(k)$ to be the probability that k hadrons of some specific type decay from one cluster, one finds that the fully inclusive correlation function (for the "non-diffractive" component) has the form [1,2]

$$C(y_1, y_2) = \frac{\langle k(k-1) \rangle}{\langle k \rangle} \left(\frac{1}{\sigma} \frac{d\sigma}{dy} \right)_{y=0} G(y_1 - y_2), \quad (1.5)$$

when y_1 and y_2 are in the central region. Here the (unrestricted) averages are

$$\langle k \rangle = \sum k p(k); \quad (1.6)$$

$$\text{and } \langle k(k-1) \rangle = \sum k(k-1) p(k). \quad (1.7)$$

The Gaussian function

$$G(y_1 - y_2) = \frac{1}{2\delta \sqrt{\pi}} \exp \left[- \frac{(y_1 - y_2)^2}{4 \delta^2} \right], \quad (1.8)$$

has an effective "correlation length" 2δ . It is particularly relevant at small values of $(y_1 - y_2)$. For pions, which comprise the bulk of the charged particles in the central region, the numerical value of δ is 0.6 to 0.9 (c.f. sect. 3.1); it is smaller for heavier particles.

In sect. 4, for semi-inclusive correlation functions in the central region, I derive the new result (eq. (4.29) of the text)

$$C_n(y_1, y_2) = A_0 \left(\frac{1}{\sigma_n} \frac{d\sigma_n}{dy} \right)_{y=0} G(y_1 - y_2) - \frac{1}{n} (1 + A_0) \left(\frac{1}{\sigma_n} \frac{d\sigma_n}{dy_1} \right) \left(\frac{1}{\sigma_n} \frac{d\sigma_n}{dy_2} \right) \quad (1.9)$$

This expression applies for $n > \frac{1}{2} \langle n \rangle$.

Quantity A_0 in eq. (1.9) is in general a function of n . Its n dependence reflects directly the structure of the internal cluster multiplicity distribution $p(k)$, as is described in detail in sect. 4. If $p(k)$ is very narrow, ^(*) A_0 is independent of n and $s[A_0 \approx \langle k(k-1) \rangle$; sect. 4.1], whereas if $p(k)$ is broad, A_0 increases considerably with n [$A_0 \approx (n-1) \langle k \rangle / \langle n \rangle$; sect. 4.2]. These conclusions are shown to be independent of assumptions concerning the n and y dependences of $\sigma_n^{-1} d\sigma_n/dy$.

From the point of view of cluster models, the new physical content of semi-inclusive data resides in the function A_0 . It is suggested, therefore, that data be fitted to eq. (1.9), and that A_0 be extracted as a function of n .

For reasons described in sect. 4.3, the n dependence of this function is more readily interpretable (and less subject to model dependent kinematical corrections) than that of $C_n(0,0)$ or of $R_n(0,0)$.

By comparing eq. (1.8) and (1.9), one may identify A_0 as

$$A_0 = \left(\frac{\langle k(k-1) \rangle}{\langle k \rangle} \right)_n$$

Thus, A_0 describes how the ratio of cluster averages varies with final state multiplicity.

In preliminary analysis of ISR correlation data along the lines of eq. (1.9), A_0 is found to vary slowly with n , if at all [8]. Thus, narrow distributions $p(k)$ are favored. The mean number of hadrons per cluster (charged plus neutral) is between 3 and 4.

(*) i.e. has very small dispersion in multiplicity about $\langle k \rangle$.

The article is organized in the following way. Because the formalism and assumptions underlying the cluster emission viewpoint have not before been published, I fill this void with a general treatment in sect. 2. In sect. 3, I present explicit expressions for isotropic cluster decay (sect. 3.1), and for independent cluster production according to a multi-peripheral-like production model (sect. 3.2). The main new phenomenological results are developed in sect. 4, to which the expert reader may wish to turn directly. Various remarks are collected in sect. 5.

2. GENERAL FORMATION

A two-step process is envisaged in which clusters of hadrons are produced according to some basic dynamical scheme, and subsequently decay into observed hadrons. Expressions are derived for cross sections, not for amplitudes. The basic dynamical scheme should contain peripheral, diffractive and non-diffractive effects and, in principle, applies throughout phase space.

Correlations among hadrons in the central region of rapidity are the main subject of this article. In keeping with the apparently energy-independent (scaling) character of fully inclusive two-particle rapidity correlation data in the central region [3-7], it is usually assumed that the dominant dynamical production mechanism in this central region is of an independent-emission or multiperipheral-type [1]. To be sure diffractive effects also contribute. For the general purposes of sect. 2, however, specification of the details of production are not necessary. General expressions will be given first and, later, in sect. 3, specific assumptions will be introduced about production and decay dynamics.

2.1 Notation and Definitions

The basic production mechanism provides several distributions. First, there are cross sections σ_N for production of N clusters as a function of N and of energy s ; $P_N \equiv \sigma_N/\sigma$. Second, the single-cluster rapidity distribution

$$\rho_N^{(1)}(s, y_c, P_T) = \frac{1}{\sigma_N} \frac{d^2 \sigma_N}{dy_c dP_T^2} \quad (2.1)$$

is to be given as a function of s , the cluster rapidity y_c , and the (whole) cluster's transverse momentum P_T . When integrated over P_T , this is the probability for finding a cluster centered at y_c in a N cluster final state.

Third, we require the two-cluster distribution

$$\begin{aligned} \rho_N^{(2)}(s, y_{c1}, y_{c2}, P_{T1}, P_{T2}, \phi) \\ = \frac{1}{\sigma_N} \frac{d^5 \sigma_N}{dy_{c1} dy_{c2} dP_{T1}^2 dP_{T2}^2 d\phi} \end{aligned} \quad (2.2)$$

Here, ϕ is the azimuthal angle between the transverse momentum vectors \vec{P}_{T1} and \vec{P}_{T2} of the two clusters.

The rapidity, transverse momenta, and azimuthal angles of hadrons are denoted by lower case symbols y , p_T and ϕ , respectively.

It would be valuable to study the p_T and ϕ dependences of rapidity correlations. These may give important information on the P_T and ϕ dependences of expression (2.2). However, in this article I am concerned only with the y correlations present after an integration has been made over all p_T and ϕ . Thus, instead of expressions (2.1) and (2.2), it is sufficient to deal with the integrated quantities

$$\rho_N^{(1)}(s, y_c) = \frac{1}{\sigma_N} \frac{d\sigma_N}{dy_c} \quad (2.3)$$

and

$$\rho_N^{(2)}(s, y_{c1}, y_{c2}) = \frac{1}{\sigma_N} \frac{d^2 \sigma_N}{dy_{c1} dy_{c2}} \quad (2.4)$$

These satisfy the integral relations

$$\int \rho_N^{(1)}(s, y_c) dy_c = N \quad (2.5)$$

and

$$\int \rho_N^{(2)}(s, y_{c1}, y_{c2}) dy_{c1} dy_{c2} = N(N-1). \quad (2.6)$$

The integrals extend over all phase-space. The clusters are assumed identical.

Disintegration of a cluster into observed hadrons of type h (e.g. charged hadrons, π^- , \bar{p} , or any other specific species) is described by function $D_n^{(1)}(y, y_c)$, normalized to unity.

$$\int D_h^{(1)}(y, y_c) dy = 1. \quad (2.7)$$

Function D_h may be different for different h. It is an inclusive quantity in the sense that

$$\langle k_h \rangle D_h^{(1)}(y, y_c) \quad (2.8)$$

is the inclusive yield in y of type h hadrons decaying from a cluster at y_c ; $\langle k_h \rangle$ is the mean number of type h hadrons which come from the cluster. Again, transverse momenta have been summed-over.

Function D is assumed here to be independent of the cluster's decay multiplicity. (This point is discussed further in sect. 3.1).

The inclusive decay of one cluster into hadrons h_1 and h_2 is described by

with

$$D_{h_1 h_2}^{(2)}(y_1, y_2; y_c) \quad (2.9)$$

$$\int dy_1 \int dy_2 D_{h_1 h_2}^{(2)} = 1.$$

The multiplicity distribution of hadrons of type h from a single basic cluster is $p(k)$. (I drop the subscript h).

$$\sum_k p(k) = 1. \quad (2.10)$$

This basic distribution is left unspecified. Its properties are to be extracted from data, insofar as is possible. The mean number of hadrons $\langle k \rangle$ (of given type h) which arise from a given basic unrestricted cluster is

$$\langle k \rangle = \sum_k k p(k), \quad (2.11)$$

and

$$\langle k(k-1) \rangle = \sum_k k(k-1) p(k). \quad (2.12)$$

The hadron inclusive spectra $\sigma_n^{-1} d\sigma_n/dy$ and $\sigma_n^{-1} d^2\sigma_n/dy_1 dy_2$ at fixed multiplicity n of hadrons (of type h), are obtained after a convolution over y_c and a sum over k and N ; for example,

$$\frac{1}{\sigma_n} \frac{d\sigma_n}{dy} = \sum_N \sum_k M_{Nn}(k) \int dy_c \rho_N^{(1)}(y_c) D^{(1)}(y, y_c) \quad (2.13)$$

The convolution over y_c follows in obvious fashion from the definitions above. The multiplicity combinations leading to $M_{Nn}(k)$ are discussed below.

2.2 Multiplicity Combinations

All clusters are assumed here to have the same decay spectrum $p(k)$, a distribution which would be measured if one were to observe a single cluster. However, a cluster is generally not observed in isolation. Rather, in dealing with a final state of fixed hadron multiplicity n , we see the results of a convolution of $p(k)$ with the cluster production distribution $P_N = \sigma_N/\sigma$.

Some general expressions for observables are derived here, for arbitrary P_N and $p(k)$. Then, in subsect. 2.2.1 special forms are chosen for $p(k)$, resulting in simplified specific formulas.

Throughout this article, symbols N , k , and n stand for the multiplicity of clusters, the multiplicity of hadrons within one cluster, and the number of hadrons of some specific type in the final state, in that order.

The probability that cluster i in an n hadron and N cluster final state decays into k_i hadrons is denoted $\tilde{p}_i(k_i; N, n)$. Thus,

$$\tilde{p}_i(k_i; N, n) = \sum_{k_N} \dots \sum_{k_2} \sum_{k_1} \prod_{j=1}^N p_j(k_j) \left\{ \sum_{j=1}^N k_j = n \right\} \quad (2.14)$$

As indicated, the $(N-1)$ summations in (2.14) are made subject to the constraint that $n = \sum_{j=1}^N k_j$. No sum is made over k_i , which is fixed.

The probability that n hadrons are produced in an N cluster final state is then

$$q_N(n) = \sum_{k_i} \tilde{p}_i(k_i; N, n) \quad (2.15)$$

It is easy to deduce that $\sum_n q_N(n) = 1$, and that

$$\langle n \rangle_N = \sum_n n q_N(n) = N \langle k \rangle \quad (2.16)$$

The net probability that n hadrons are produced, after summation over N , is

$$Q_n = \sum_N P_N q_N(n) \equiv \sigma_n / \sigma \quad (2.17)$$

$$\langle n \rangle = \sum_n n Q_n = \langle N \rangle \langle k \rangle \quad (2.18)$$

In an n hadron, N cluster final state, the joint probability that cluster i decays into k_i hadrons and that cluster j decays into k_j hadrons is ($i \neq j$)

$$J_{ij}(k_i, k_j; N, n) = \sum_{k_N} \dots \sum_{k_2} \sum_{k_1} \prod_{\ell=1}^N p_\ell(k_\ell) \quad (2.19)$$

$$\{ N = \sum_{\ell} k_\ell \} .$$

On the right, no sums are made over k_i and k_j , which are fixed. From the definitions it is clear that

$$\tilde{p}_i(k_i; N, n) = \sum_{k_j} J_{ij}(k_i, k_j; N, n) \quad (2.20)$$

In later expressions it will be useful to have deduced several intermediate quantities from the above definitions.

In an N cluster, n hadron final state, the mean number of hadrons per cluster is

$$\begin{aligned} \langle k \rangle_{N,n} &\equiv (q_N(n))^{-1} \sum_{k_i} k_i \tilde{p}_i(k_i; N, n) \\ &= n/N. \end{aligned} \quad (2.21)$$

Likewise

$$\langle k(k-1) \rangle_{N,n} \equiv (q_N(n))^{-1} \sum_{k_i} k_i(k_i-1) \tilde{p}_i(k_i; N, n) \quad (2.22)$$

These are not directly observable quantities since clusters themselves are not seen.

In an n hadron final state (after a sum over the unobservable cluster spectrum P_N), the mean number of hadrons per cluster is

$$\langle k \rangle_n = Q_n^{-1} \sum_N P_N \sum_{k_i} k_i \tilde{p}_i(k_i; N, n) \quad (2.23)$$

Moreover,

$$\langle k(k-1) \rangle_n = Q_n^{-1} \sum_N P_N \sum_{k_i} (k_i)(k_i-1) \tilde{p}_i(k_i; N, n) \quad (2.24)$$

Both $\langle k \rangle_n$ and $\langle k(k-1) \rangle_n$ are, in principle, functions of n . Their n dependence gives information on $p(k)$, as will be described below.

In a fully inclusive measurement (sums over both N and n), the mean number of hadrons per cluster is

$$\begin{aligned} \langle k \rangle_{\text{incl}} &= \sum_n \sum_N P_N \sum_{k_i} k_i \tilde{p}_i(k_i; N, n) \\ &= \sum_N P_N \left(\sum_{k_i} k_i p_i(k_i) \right) = \langle k \rangle \quad (2.25) \end{aligned}$$

This is identical to the unrestricted quantity defined in eq. (2.11).

$$\begin{aligned} \langle k(k-1) \rangle_{\text{incl}} &= \sum_n \sum_N P_N \sum_{k_i} k_i(k_i-1) \tilde{p}_i(k_i; N, n) \\ &= \sum_N P_N \sum_{k_i} k_i(k_i-1) p_i(k_i) = \langle k(k-1) \rangle \quad (2.26) \end{aligned}$$

Thus, we see that from fully inclusive data one measures in principle the averages within a cluster. Semi-inclusive data provide the n dependences of these cluster averages.

Expressions for $\langle n \rangle_N$ and $\langle n \rangle$ were given above, in eq. (2.16) and (2.18). Quantities involving $n(n-1)$ are more involved.

$$\begin{aligned} n^2 q_N(n) &= \left(\sum_{j=1}^N k_j \right)^2 q_N(n) \\ &= N \sum_{k_i} k_i^2 \tilde{p}_i(k_i; N, n) \\ &\quad + N(N-1) \sum_{k_i} \sum_{k_j} k_i k_j J_{ij}(k_i, k_j; N, n) \end{aligned} \quad (2.27)$$

The last equality is obtained after a little algebra from the definitions given in eqs. (2.14), (2.15) and (2.19).

Upon summing this last equation over n , we find that at fixed N ,

$$\langle n(n-1) \rangle_N = N \langle k(k-1) \rangle + N(N-1) \langle k \rangle^2 \quad (2.28)$$

Moreover,

$$\langle n(n-1) \rangle = \langle N \rangle \langle k(k-1) \rangle + \langle N(N-1) \rangle \langle k \rangle^2 \quad (2.29)$$

and

$$\begin{aligned} f_2 &\equiv \langle n(n-1) \rangle - \langle n \rangle^2 \\ &= \langle N \rangle \langle k(k-1) \rangle + \{ \langle N(N-1) \rangle - \langle N \rangle^2 \} \langle k \rangle^2 \end{aligned}$$

Defining $F_2 = \langle N(N-1) \rangle - \langle N \rangle^2$, one may rewrite the last equation as

$$f_2 = \langle N \rangle \langle k(k-1) \rangle + \langle k \rangle^2 F_2 \quad (2.30)$$

2.2.1 Specific forms for $p(k)$

2.2.1a Delta function

Perhaps one case of physical interest is that in which the basic clusters have a very narrow multiplicity distribution [11]. In the extreme, we may assume a fixed cluster multiplicity, such that

$$p(k) = \delta(k-k_0) \quad . \quad (2.31)$$

If so, $\langle k \rangle = \langle k \rangle_n = k_0$ and $\langle k(k-1) \rangle_n = \langle k(k-1) \rangle = k_0(k_0-1)$.

Moreover,

$$\tilde{p}_i(k_i; N, n) = \delta(n-Nk_0) \delta(k_i-k_0); \quad (2.32a)$$

$$q_N(n) = \delta(n-Nk_0) = \frac{1}{k_0} \delta\left(N - \frac{n}{k_0}\right); \quad (2.32b)$$

$$Q_n = \frac{1}{k_0} P_{\left(N=\frac{n}{k_0}\right)}; \quad (2.32c)$$

and

$$J_{ij}(k_i, k_j; N, n) = \delta(n-Nk_0) \delta(k_i-k_0) \delta(k_j-k_0) \quad . \quad (2.32d)$$

2.2.1b Poisson Form for p(k)

A second case of interest, particularly because it allows simple expressions in closed form, is that in which p(k) has a Poisson form:

$$p(k) = e^{-z} \frac{z^k}{k!} \quad . \quad (2.33)$$

Here $z \equiv \langle k \rangle$.

Noting that a product of N Poisson distributions is itself a Poisson distribution characterized by a mean N times as great as that of the single cluster, one obtains

$$\tilde{p}_i(k_i; N, n) = \frac{e^{-Nz} (N-1)^{n-k_i} z^n}{k_i! (n-k_i)!}; \quad (2.34a)$$

$$q_N(n) = \frac{e^{-Nz} z^n}{n!}; \quad (2.34b)$$

$$Q_n = \left(\sum_N P_N q_N(n) \right) (= \sigma_n / \sigma); \quad (2.34c)$$

and

$$J_{12}(k, \ell; N, n) = \frac{e^{-Nz} z^n (N-2)^{n-k-\ell}}{k! \ell! (n-k-\ell)!} \quad . \quad (2.34d)$$

Furthermore, after trivial algebra, one derives

$$\langle k \rangle_n = \frac{\langle k \rangle \sigma_{n-1}}{\sigma_n} \quad (2.36)$$

$$\langle k(k-1) \rangle_{N,n} = \frac{n(n-1)}{N^2} \quad (2.36)$$

$$\langle k(k-1) \rangle_n = \frac{\langle k \rangle^2 \sigma_{n-2}}{\sigma_n} \quad (2.37)$$

It will be noted that eq. (2.37) is valid for an arbitrary choice of P_N , the probability function for production of N clusters.

The derivation of eq. (2.37) is recorded here inasmuch as it is a prototype of other results important in sect. 3. From (2.22) and (2.34a), one may write

$$q_N(n) \langle k(k-1) \rangle_{N,n} = \sum_{k=2}^n k(k-1) \frac{e^{-Nz} (N-1)^{n-k} z^n}{k! (n-k)!}$$

($k \rightarrow k-2$)

$$\begin{aligned} &= \frac{e^{-Nz} z^n}{(n-2)!} \sum_{k=0}^{n-2} \frac{(N-1)^{n-2-k} (n-2)!}{k! (n-2-k)!} \\ &= \frac{e^{-Nz} z^n}{(n-2)!} N^{n-2} \quad (2.38) \end{aligned}$$

Then

$$\begin{aligned} \langle k(k-1) \rangle_n &\equiv Q_n^{-1} \sum_N P_N q_N(n) \langle k(k-1) \rangle_{N,n} \\ &= Q_n^{-1} z^2 \sum_N P_N q_N(n-2) \\ &= z^2 Q_{n-2} / Q_n \equiv \langle k \rangle^2 \sigma_{n-2} / \sigma_n \end{aligned}$$

2.3 Inclusive Distributions

It is straightforward to combine the expressions given in subsect. 2.1 and 2.2 so as to obtain the inclusive single and two-particle rapidity distributions $\sigma_n^{-1} d\sigma_n/dy$ and $\sigma_n^{-1} d^2\sigma_n/dy_1 dy_2$ at fixed multiplicity n of final hadrons.

After the sum over N identical clusters, the inclusive yield of hadrons in an N cluster, n hadron final state is

$$\frac{1}{\sigma_{N,n}} \frac{d\sigma_{N,n}}{dy} = [q_N(n)]^{-1} \int dy_c \rho_N^{(1)}(y_c) dy_c \sum_k \tilde{p}(k;N,n) D^{(1)}(y,y_c) . \quad (2.39)$$

After a sum over all cluster multiplicities,

$$\frac{1}{\sigma_n} \frac{d\sigma_n}{dy} = Q_n^{-1} \sum_N P_N \int dy_c \rho_N^{(1)}(y_c) \sum_k \tilde{p}(k;N,n) D^{(1)}(y,y_c) . \quad (2.40)$$

Upon integration over y and y_c, this last expression gives n, as required. Thus,

$$\begin{aligned} \int dy \left(\frac{1}{\sigma_n} \frac{d\sigma_n}{dy} \right) &= Q_n^{-1} \sum_N P_N \sum_k \tilde{p}(k;N,n) \\ &= n Q_n^{-1} \sum_N P_N q_N(n) \equiv n . \end{aligned} \quad (2.41)$$

The last equalities are obtained by using eq. (2.21).

The fully inclusive y distribution is

$$\begin{aligned} \frac{1}{\sigma} \frac{d\sigma}{dy} &= \frac{1}{\sigma} \sum_n \frac{d\sigma_n}{dy} \\ &= \sum_n \sum_N P_N \int dy_c \rho_N^{(1)}(y_c) \sum_k \tilde{p}(k;N,n) D^{(1)}(y,y_c) \\ &= \langle k \rangle \sum_N P_N \int dy_c \rho_N^{(1)}(y_c) D^{(1)}(y,y_c) . \end{aligned} \quad (2.42)$$

The two-particle inclusive distribution receives contributions from two sources. Both final hadrons may originate from the same cluster, or each may come from a different cluster. Thus, there are two terms:

$$\begin{aligned} \frac{1}{\sigma_n} \frac{d^2\sigma_n}{dy_1 dy_2} &= Q_n^{-1} \sum_N P_N \int dy_c \rho_N^{(1)}(y_c) D^{(2)}(y_1, y_2; y_c) \sum_k \tilde{p}(k;N,n) \\ &+ Q_n^{-1} \sum_N P_N \iint dy_{c1} dy_{c2} \rho_N^{(2)}(y_{c1}, y_{c2}) D^{(1)}(y_1, y_{c1}) D^{(1)}(y_2, y_{c2}) \\ &\sum_{k_2} \sum_{k_1} k_1 k_2 J_{12}(k_1, k_2; N, n) . \end{aligned} \quad (2.43)$$

By virtue of eq. (2.27), the integral of (2.43) over y_1 and y_2 , gives $n(n-1)$ as required. Thus,

$$\begin{aligned}
 & \iint dy_1 dy_2 \frac{1}{\sigma_n} \frac{d^2 \sigma_n}{dy_1 dy_2} \\
 &= Q_n^{-1} \sum_N P_N \sum_k k(k-1) \tilde{p}(k;N,n) \\
 &+ Q_n^{-1} \sum_N P_N N(N-1) \sum_{k_2} \sum_{k_1} k_1 k_2 J_{12}(k_1, k_2; N, n) \\
 &= n(n-1) Q_n^{-1} \sum_N P_N q_N(n) \equiv n(n-1) .
 \end{aligned} \tag{2.44}$$

The fully inclusive two particle rapidity distribution is

$$\begin{aligned}
 \frac{1}{\sigma} \frac{d^2 \sigma}{dy_1 dy_2} &= \frac{1}{\sigma} \sum_n \frac{d^2 \sigma_n}{dy_1 dy_2} \\
 &= \langle k(k-1) \rangle \sum_N P_N \int dy_c \rho_N^{(1)}(y_c) D^{(2)}(y_1, y_2; y_c) \\
 &+ \langle k \rangle^2 \sum_N P_N \iint dy_{c1} dy_{c2} \rho_N^{(2)}(y_{c1}, y_{c2}) D^{(1)}(y_1, y_{c1}) D^{(1)}(y_2, y_{c2})
 \end{aligned} \tag{2.45}$$

The semi-inclusive correlation function $C_n(y_1, y_2)$ is defined as

$$C_n(y_1, y_2) = \frac{1}{\sigma_n} \frac{d^2 \sigma_n}{dy_1 dy_2} - \frac{1}{\sigma_n^2} \frac{d\sigma_n}{dy_1} \frac{d\sigma_n}{dy_2} . \tag{2.46}$$

I rewrite this as a sum of two terms in order to distinguish the rapidity correlations arising from within one cluster from those contributions to C_n arising from other sources. Thus,

$$C_n(y_1, y_2) \equiv C_n^{(c)}(y_1, y_2) + C_n^{(r)}(y_1, y_2) . \tag{2.47}$$

Rapidity correlations arising from one cluster provide the function

$$C_n^{(c)}(y_1, y_2) = Q_n^{-1} \sum_N P_N \int dy_c \rho_N^{(1)}(y_c) D^{(2)}(y_1, y_2; y_c) \sum_k k(k-1) \tilde{p}(k; N, n) \quad (2.48)$$

The remaining contribution to C_n is the difference

$$\begin{aligned} C_n^{(r)}(y_1, y_2) &= Q_n^{-1} \sum_N P_N \iint dy_{c1} dy_{c2} \rho_N^{(2)}(y_{c1}, y_{c2}) D^{(1)}(y_1, y_{c1}) D^{(1)}(y_2, y_{c2}) \\ &\quad * \sum_{k_2} \sum_{k_1} k_1 k_2 J_{12}(k_1, k_2; N, n) \\ &\quad - Q_n^{-2} \sum_N P_N \int dy_{c1} \rho_N^{(1)}(y_{c1}) D^{(1)}(y_1, y_{c1}) \sum_k k \tilde{p}(k; N, n) \\ &\quad * \sum_M P_M \int dy_{c2} \rho_M^{(1)}(y_{c2}) D^{(1)}(y_2, y_{c2}) \sum_k k \tilde{p}(k; M, n) \end{aligned} \quad (2.49)$$

In order to reduce eqs. (2.40), (2.43), (2.48) and (2.49) to expressions which may be compared with data, a simple parametrization must be given for the cluster production distributions $\rho_N^{(1)}(y_c)$ and $\rho_N^{(2)}(y_{c1}, y_{c2})$ and for the decay functions $D^{(1)}$ and $D^{(2)}$. These subjects are treated in sect. 3.

3. CLUSTER DECAY AND PRODUCTION DYNAMICS

The properties of the clusters themselves are assumed to be energy independent. In particular, the multiplicity distribution $p(k)$ and the decay spectra, $D^{(1)}(y, y_c)$ and $D^{(2)}(y_1, y_2; y_c)$, are all taken to be s -independent. Any important s dependence in data is presumed to be associated with production dynamics. (Some s -dependence, however, may be associated with phase-space effects, in the sense that, for given n , if s is too small, clusters may not be fully developed).

3.1 Cluster Decay

If (\vec{q}, ω) denotes the four-vector momentum in the cluster rest frame, and y is rapidity in that frame, then, after integration over azimuthal angle ϕ , one obtains the transformation of variables:

$$\frac{d^3\vec{q}}{\omega} = \frac{2\pi dq^2 dy}{\cosh^2 y} . \quad (3.1)$$

Here $q = |\vec{q}|$.

Denoting an average decay distribution in the cluster rest frame by $D(\vec{q})$, one may write

$$\frac{dD}{dy} = 2\pi(\cosh y)^{-2} \int dq^2 D(\vec{q}) . \quad (3.2)$$

In general, D may depend on $\cos\theta$ (i.e. on y). However, the common assumption is made now that cluster decay is isotropic in the cluster rest frame: $D(\vec{q}) \rightarrow D(q)$. Setting $r = q/\langle q_k \rangle$, we obtain [13]

$$\frac{dD}{dy} = \frac{2\pi\langle q_k \rangle^2}{\cosh^2 y} I(y, \mu, \langle q_k \rangle); \quad (3.3a)$$

with

$$I(y, \mu, \langle q_k \rangle) = \int_{L_1}^{L_2} dr D(r) . \quad (3.3b)$$

In eq. (3.3), $\langle q_k \rangle$ is the average momentum of a decay hadron (of given type) in a k hadron decay of the cluster. The lower and upper limits of integration are

$$L_1 = \left(\frac{\mu \sinh y}{\langle q_k \rangle} \right)^2 ; \quad (3.4a)$$

and

$$L_2 = \frac{1}{4M^2 \langle q_k \rangle^2} \left\{ (M^2 - (\mu + M_r)^2) (M^2 - (\mu - M_r)^2) \right\} \quad (3.4b)$$

M is the cluster mass μ is the mass of the decay hadron under consideration; and M_r is the minimum mass of the set of $(k-1)$ particles remaining from the original cluster [$M_r = (k-1)\mu$ if all particles in the cluster have the same mass].

All dependence of dD/dy on multiplicity k and on decay particle type is contained in the integral factor $I(y, \mu, \langle q_k \rangle)$.

The value of $\langle q_k \rangle$ is related experimentally to the observed mean transverse momentum $\langle p_{Tn} \rangle$ of hadrons in an n hadron final state. At 205 GeV/c, $\langle p_{Tn} \rangle$ shows little n dependence over the (wide) range of n values, from (negative multiplicity) $n = 2$ to 7 [14]. Therefore, $\langle q_k \rangle$ can be assumed here to be roughly independent of k . Thus, to the same approximation, $D(y, y_c)$ is independent of cluster multiplicity k .

For pions, $(\mu/\langle p_T \rangle)^2 \lesssim 0.25$. For not too large k , one may then set $L_1 = 0$ and $L_2 = \infty$ in eq. (3.3b). With this simplification and normalized to unity,

$$D(y_1, y_c) = \frac{0.5}{\cosh^2(y-y_c)} \approx \frac{1}{\delta\sqrt{2\pi}} \exp\left[-\frac{(y-y_c)^2}{2\delta^2}\right]. \quad (3.5)$$

The Gaussian form is a good numerical approximation to $\cosh^{-2}y$, if dispersion [13]

$$\delta \approx 0.9 \quad .$$

It will be noted, however, that additional y dependence is present to the extent that $(\mu/\langle p_T \rangle)$ is non-zero. The effect is to cut-off $D(y_1, y_c)$ at large $|y-y_c|$ faster than $\cosh^{-2}(y-y_c)$, and thus to reduce the effective dispersion below $\delta \approx 0.9$. For example, the value of δ_p (for protons) should be less than that of δ_π . In fig. 2, a numerical study of these effects is presented. Clusters are allowed to decay isotropically via pure phase-space into four pions or three pions plus one nucleon. The numerical results are compared with Gaussian curves. The effective dispersions of the pion and baryon distributions are 0.70 and 0.36, respectively.

Comparison with data is the best test of whether isotropic decay is a sensible approximation. At the fully inclusive level, it does seem in fact that the shape of $C(y_1, y_2)$ at small $\Delta y = |y_1 - y_2|$ is in keeping with expectations of such a decay scheme [1,2]. However, the full range of y is not large, even at ISR energies, and some s -dependence of the effective dispersion of $C(y_1, y_2)$ might be discerned in the Pisa-Stony Brook data [4].

Perhaps the reason for success is simply that clusters have fairly low mass (1 to 2 GeV) and spin. Polarization effects and elongation may therefore be relatively insignificant. A more detailed examination of the isotropic decay guess, at least of its n independence, is provided by the study of $C_n(y_1, y_2)$, as described below.

For the two-hadron decay function, the simplest postulate is

$$D^{(2)}(y_1, y_2; y_c) = D^{(1)}(y_1, y_c) D^{(1)}(y_2, y_c) \quad (3.6)$$

This expresses independent decay. The reliability of eq. (3.6) may be studied in a Monte Carlo calculation, in which energy and momentum conservation are fully respected. As demonstrated by fig. 3, the approximation is not unreasonable.

After trivial algebraic manipulation, we can rewrite eq. (3.6) as

$$D^{(2)}(y_1, y_2; y_c) = \frac{1}{2\pi\delta^2} \exp \left[-\frac{1}{4\delta^2} (y_1 - y_2)^2 - \frac{1}{\delta^2} \left(\frac{1}{2}(y_1 + y_2) - y_c \right)^2 \right]. \quad (3.7)$$

Note that

$$\int dy_c D^{(2)}(y_1, y_2; y_c) = \frac{1}{2\delta\sqrt{\pi}} \exp \left[-\frac{1}{4\delta^2} (y_1 - y_2)^2 \right]. \quad (3.8)$$

Upon inserting eq. (3.7) into eq. (2.48), we conclude that the correlation function $C_n^{(c)}(y_1, y_2)$ has the general form of a function of the difference $(y_1 - y_2)$ times another function of the sum $(y_1 + y_2)$.

$$C_n^{(c)}(y_1, y_2) = G(y_1 - y_2) \sum_N \sum_k f_N((y_1 + y_2), Y) M_{N,n}^{(2)}(k)$$

where

$$G(y_1 - y_2) = \frac{1}{2\delta\sqrt{\pi}} \exp \left[-\frac{1}{4\delta^2} (y_1 - y_2)^2 \right]; \quad (3.10)$$

and

$$f_N((y_1 + y_2), Y) = \frac{1}{\delta\sqrt{\pi}} \int dy_c \rho_N^{(1)}(y_c) \exp \left[-\frac{1}{\delta^2} \left(\frac{1}{2}(y_1 + y_2) - y_c \right)^2 \right] \quad (3.11)$$

($Y = \log s$)

3.2 Production Dynamics

3.2.1 Qualitative Remarks

Distinct reaction mechanisms, with different characteristic properties, have been identified and to some extent isolated in the enlarged phase space available at NAL and ISR. Among these one may cite single inelastic peripheral proton scattering (diffraction dissociation), production at large p_T , and central region production.

In the central region of rapidity space, the main features of data are roughly consistent with the hypothesis that the basic dynamics is one of purely short-range order, although long-range correlation effects are no doubt present also (if for no other reason, from the tail of diffractive effects) [1]. Dominant short range order (or pure short-range correlations) predicts a scaling plateau in the central region ($\sigma^{-1} d\sigma/dy \rightarrow \text{constant}$, independent of y and s). While this expectation is not fully supported at ISR, even for pion production [15], one may view the data as suggesting its asymptotic validity. The more crucial prediction of short range order is that the inclusive correlation function $C(y_1, y_2)$ should (1) be s independent, (2) be a function only of $(y_1 - y_2)$ and (3) decrease rapidly in magnitude as $|y_1 - y_2|$ increases. These expectations are consistent with published data for the ratio [3-7]

$$R(y_1, y_2) = C(y_1, y_2) / \frac{1}{\sigma^2} \left(\frac{d\sigma}{dy_1} \right) \left(\frac{d\sigma}{dy_2} \right),$$

as long as both y_1 and y_2 are restricted to $|y_i| < 1$. To be sure, more detailed investigations would be helpful on the s dependence of $C(y_1, y_2)$ for hadrons of specific type (π , K , p , etc.) and well defined p_T .

3.2.2 Several Mechanisms

As summarized above, one may accept as a working hypothesis at present that the controlling mechanism in the central region is one for which correlations are purely of short range character. Nevertheless, the existence of other mechanisms affects the interpretation of correlation functions in an important way [1,2].

The inelastic cross section for multiplicity n is written as the sum of (at least) two contributions:

$$\sigma_n = \sigma_n^{SR} + \sigma_n^{\text{other}}, \quad (3.13)$$

where σ_n^{SR} is that part of n hadron inelastic cross section attributed to the short-range dynamics. The remainder, σ_n^{other} , is made up largely of inelastic diffraction, and thus one often identifies $\sigma_n^{\text{other}} = \sigma_n^D$. A similar decomposition gives

$$\frac{1}{\sigma_n} \frac{d\sigma_n}{dy} = \alpha_n^{SR} \frac{1}{\sigma_n^{SR}} \frac{d\sigma_n^{SR}}{dy} + \alpha_n^D \frac{1}{\sigma_n^D} \frac{d\sigma_n^D}{dy} \quad (3.14)$$

and

$$C_n(y_1, y_2) = \alpha_n^{SR} C_n^{SR}(y_1, y_2) + \alpha_n^D C_n^D(y_1, y_2) + \alpha_n^D \alpha_n^{SR} C_n^{\text{Cross}}(y_1, y_2). \quad (3.15)$$

Here $\alpha_n^{SR} = \sigma_n^{SR}/\sigma_n$; $\alpha_n^D = \sigma_n^D/\sigma_n$; $C_n^{SR}(y_1, y_2)$ and $C_n^D(y_1, y_2)$ are the rapidity correlation functions at fixed n for the purely non-diffractive and diffractive mechanisms, respectively. For example,

$$C_n^{SR} = \frac{1}{\sigma_n^{SR}} \frac{d^2 \sigma_n^{SR}}{dy_1 dy_2} - \left(\frac{1}{\sigma_n^{SR}} \right)^2 \frac{d\sigma_n^{SR}}{dy_1} \frac{d\sigma_n^{SR}}{dy_2}. \quad (3.16)$$

$$C_n^{\text{Cross}}(y_1, y_2) = \left[\frac{1}{\sigma_n^{SR}} \frac{d\sigma_n^{SR}}{dy_1} - \frac{1}{\sigma_n^D} \frac{d\sigma_n^D}{dy_1} \right] \times \left[1 \leftrightarrow 2 \right]. \quad (3.17)$$

By dropping multiplicity subscript n in eqs. (3.15-3.17), one obtains equations for the decomposition of the fully inclusive correlation function $C(y_1, y_2)$. As in the fully inclusive case, even if both C_n^{SR} and C_n^D were both of a purely short range character (vanish for $\Delta y = |y_1 - y_2| \gg \lambda$), the presence of C_n^{Cross} gives a long-range correlation component to C_n .

Because $\sigma_D \approx 7\text{mb}$, and $(\sigma^D)^{-1} d\sigma^D/dy$ can be shown theoretically at least, to be substantial even near $y \approx 0$, an understanding of $C(y_1, y_2)$ requires proper understanding of each of the three terms in eq. (3.15). Stated

otherwise, fits to fully inclusive correlation data require model-dependent assumptions about the non-short-range order part of σ^{inel} , and about its separation from σ^{SR} . The semi-inclusive data offer a significant advantage in this regard. For large enough n , contributions to σ_n from the diffractive term become negligible. Therefore, semi-inclusive correlations at fixed large n may offer cleaner insight into the dynamical mechanism which dominates production in the central region. Arguments given below suggest that only the first term in eq. (3.15) is important for $n \gtrsim 1/2 \langle n \rangle$.

A separation of σ_n and of $d\sigma_n/dy$ into "diffractive" and "non-diffractive" parts may be relatively clean at small n , but it is necessarily ambiguous at larger n where mechanisms overlap in phase space. Nevertheless, adopting reasonable operational procedures, experimenters using NAL data estimate [16] that $\sigma_n^{\text{D}}/\sigma_n < 20\%$ for $n \approx 1/2 \langle n \rangle$ and $< 10\%$ for $n \approx \langle n \rangle$. Similar figures may be obtained theoretically, for example, from a model [17] in which one assumes that the diffractive mechanism is represented by Pomeron exchange, with the Pomeron-proton subamplitude being non-diffractive in character. For small n , $d\sigma_n^{\text{D}}/dy$ surely peaks near $y = \pm \log \sqrt{s}$. However, as n increases, the chance increases that a diffractively produced system will populate the region near $y \approx 0$, perhaps even roughly uniformly [1]. This, taken together with the normalization condition (*) [eq. (1.2)], suggests that the difference given in square brackets in eq. (3.17) vanishes in the central region as n increases. Combining these two arguments (σ_n and $d\sigma_n/dy$) and supported by model calculations [18], I find that the net cross-term $\alpha_n^{\text{D}} \alpha_n^{\text{SR}} C_n^{\text{Cross}}$ in eq. (3.15) may be ignored for $n \gtrsim 1/2 \langle n \rangle$. Likewise, $\alpha_n^{\text{D}} C_n^{\text{D}}$ should be ignorable for $y_1 \gtrsim y_2 \gtrsim 0$ when $n \gtrsim 1/2 \langle n \rangle$. Thus, attention is henceforth directed solely to the pure short-range contribution to C_n , and conclusions are restricted to $n \gtrsim 1/2 \langle n \rangle$. The superscript SR is hereforth dropped.

3.2.3 Multiperipheral Production of Clusters

The prototype of pure-short-range order models is the multiperipheral model [19]. In the simplest versions, in which pions are emitted singly and all exchanged trajectories are equal, zero correlation is predicted

(*) The normalization condition applies separately to each component of σ_{inel} .

asymptotically (i.e. $R(0,0) \stackrel{\sim}{=} 0$). Positive correlation would result if resonances were emitted instead of single pions. Following this kind of argument, we invoke the multiperipheral approach as the basic dynamical mechanism for cluster production in the central region [1,20-22]. Clusters of hadrons (resonance-like objects) are emitted more or less independently, and correlations between observed hadrons are explained as owing to the existence of these clusters. The positivity of $R(0,0)$ and the specific rapidity dependence of $R(y_1-y_2)$ are to be associated with properties of clusters.

The simplest multiperipheral amplitude is one in which all exchanged trajectories are identical, and in which Pomeron exchange ($\alpha_p(0) = 1$) is excluded. If we assume that identical clusters are produced by such a mechanism, then in an over idealized high-energy limit [23],

$$P_N(s) = \sigma_N / \sigma = [\exp(-\langle N \rangle)] \langle N \rangle^N / N! \quad (3.18)$$

with

$$\langle N \rangle = BY \equiv B \log s \quad (3.19)$$

and

$$\rho_N^{(1)}(y) = \frac{1}{\sigma_N} \frac{d\sigma_N}{dy} = \frac{N}{Y} \quad (3.20)$$

These equations give a Poisson distribution of cluster multiplicity $N(F_2 = 0)$, and provide a single cluster density $\rho_N^{(1)}(y)$ which is a uniform plateau in y extending over the full range $-\frac{Y}{2} \leq y \leq \frac{Y}{2}$, for each N . The plateau height at fixed N falls as Y^{-1} .

The fully inclusive y spectrum is

$$\frac{1}{\sigma} \frac{d\sigma}{dy} = \frac{1}{Y\sigma} \sum_N N \sigma_N = \frac{\langle N \rangle}{Y} \equiv B. \quad (3.21)$$

Owing to energy-momentum conservation, if nothing else, the production distribution P_N will no doubt be cut-off faster than Poisson at large N . For this, and other reasons, it is useful to keep an open-mind about P_N . Thus, the Poisson form given in eq. (3.18) is not employed here explicitly.

The extreme single-cluster rapidity distribution, eq. (3.20), is also unnecessarily specific. Doubtlessly, as N increases, there is shrinkage of the effective interval in y over which clusters spread. To maintain the exact normalization condition

$$\int \rho_N^{(1)}(y_c) dy_c = N \quad (3.22)$$

the height should then grow faster than N . Expression (3.20) is also incompatible with energy conservation, coupled with the (experimental) requirement that $\langle p_{Tn} \rangle$ be nearly independent of n (c.f. sect. 4.3). Keeping options open and avoiding unnecessary assumptions, I write

$$\rho_N^{(1)}(y_c) = N g_N(Y, y_c) , \quad (3.23)$$

where properties of the function g_N will be discussed as needed. Factoring out N in eq. (3.23) takes care of the most prominent dependence on N .

Because the clusters are produced essentially independently, the two cluster production density at fixed N is

$$\rho_N^{(2)}(y_{c1}, y_{c2}) = \frac{N-1}{N} \rho_N^{(1)}(y_{c1}) \rho_N^{(1)}(y_{c2}) . \quad (3.24)$$

It satisfies the exact normalization condition

$$\int \rho_N^{(2)} dy_{c1} dy_{c2} = N(N-1) . \quad (3.25)$$

In case $\rho_N^{(1)} = N/Y$, one obtains

$$\rho_N^{(2)}(y_{c1}, y_{c2}) = N(N-1)/Y^2 , \quad (3.26)$$

and

$$\frac{1}{\sigma} \frac{d^2\sigma}{dy_1 dy_2} = \frac{1}{\sigma} \sum_N \sigma_N \rho_N^{(2)} = \frac{\langle N(N-1) \rangle}{Y^2} = B^2 + F_2/Y^2 . \quad (3.27)$$

3.3 Semi-Inclusive Distributions

In this section, I collect expressions for semi-inclusive rapidity distributions, based upon the equations for isotropic cluster decay and

independent cluster production derived in sect. 3.1 and 3.2. I define, first,

$$H_N^{(1)}(Y, Y) = \int dy_c g_N(Y, Y_c) D^{(1)}(Y, Y_c); \quad (3.28)$$

and

$$\begin{aligned} H_N^{(2)}(Y, (Y_1 + Y_2)) \\ = \frac{1}{\delta\sqrt{\pi}} \int dy_c g_N(Y, Y_c) \exp \left[\frac{-1}{\delta^2} \left(y_c - \frac{1}{2} (Y_1 + Y_2) \right)^2 \right] \end{aligned} \quad (3.29)$$

Function $g_N(Y, Y_c)$ is given in eq. (3.23), and $D^{(1)}(Y, Y_c)$ is given explicitly by eq. (3.5). Note that both $H^{(1)}$ and $H^{(2)}$ are obtained by convolution of g_N with a Gaussian form. The dispersion of this Gaussian is δ for $H^{(1)}$, and $\delta/\sqrt{2}$ for $H^{(2)}$.

The single- and two-hadron semi-inclusive spectra are therefore

$$\frac{1}{\sigma_n} \frac{d\sigma_n}{dy} = Q_n^{-1} \sum_N P_N H_N^{(1)}(Y, Y) \sum_k \tilde{p}(k; N, n) \quad (3.30)$$

and

$$\begin{aligned} \frac{1}{\sigma_n} \frac{d^2\sigma_n}{dy_1 dy_2} &= G(Y_1 - Y_2) Q_n^{-1} \sum_N P_N H_N^{(2)}(Y, Y_1 + Y_2) \sum_k \tilde{p}(k; N, n) \\ &+ Q_n^{-1} \sum_N P_N H_N^{(1)}(Y, Y_1) H_N^{(1)}(Y, Y_2) \\ &* \sum_{k_2} \sum_{k_1} k_1 k_2 J_{12}(k_1, k_2; N, n). \end{aligned}$$

The Gaussian function $G(Y_1 - Y_2)$ is given by eq. (3.10), and the multiplicity factors were explained in sect. 2.2.

Although simplified somewhat from their most general expressions (eq. (2.40) and eq. (2.43)), the present forms for $d\sigma_n/dy$ and $d^2\sigma_n/dy_1 dy_2$ are still too complicated for direct confrontation with data. In order to illustrate more explicitly the physical content of semi-inclusive correlations, I will choose rather specific (extreme) forms for the single cluster density $\rho_N^{(1)}(y_c)$ and for the single cluster multiplicity distribution

$p(k)$. These simplifications are made in sect. 4 and lead to expressions whose n and y dependences are more transparent.

4. PRACTICAL PHENOMENOLOGY

In this section, simple expressions are derived for semi-inclusive rapidity spectra and correlation functions. Although based on rather naive approximations for the internal cluster multiplicity distribution $p(k)$ and for the single cluster rapidity spectra $\rho_N^{(1)}(y_c)$, they have the virtues of being simple enough for comparison with data and of illustrating a range of possibilities.

4.1 Narrow Cluster Multiplicity Distribution

The simplest situation [11] arises when $p(k) = \delta(k-k_0)$ and $\rho_N^{(1)}(y_c) = N/Y$ [c.f. subsect. 2.2.1 and eqs. (3.20) and (3.26)]. Although extreme, the case $p(k) = \delta(k-k_0)$ may be taken as representative of situations in which the internal cluster multiplicity distribution is "narrow". The choice $\rho_N^{(1)}(y_c) = N/Y$ is the (very) asymptotic multiperipheral expectation. One obtains

$$\frac{1}{\sigma_n} \frac{d\sigma_n}{dy} = \frac{n}{Y} \quad (4.1)$$

$$\frac{1}{\sigma_n} \frac{d^2\sigma_n}{dy_1 dy_2} = \frac{n(k_0-1)}{Y} G(y_1-y_2) + \frac{n(n-k_0)}{Y^2} \quad (4.2)$$

$$C_n(y_1, y_2) = \frac{n(k_0-1)}{Y} G(y_1-y_2) - \frac{nk_0}{Y^2} . \quad (4.3)$$

The Gaussian function $G(y_1-y_2)$ is given by eq. (3.10).

Rewritten in a form which appears more general, the correlation function becomes

$$C_n(y_1, y_2) = (k_0-1) \left(\frac{1}{\sigma_n} \frac{d\sigma_n}{dy} \right)_0 G(y_1-y_2) - \frac{k_0}{n} \left(\frac{1}{\sigma_n} \frac{d\sigma_n}{dy_1} \right) \left(\frac{1}{\sigma_n} \frac{d\sigma_n}{dy_2} \right) . \quad (4.4)$$

These expressions are all independent of whatever arbitrary form is chosen for P_N . Although eq. (4.4) was derived under the assumption that both y_i are in the central region, we may conjecture that it remains valid outside this region, provided that we employ a realistic (i.e. the observed) y dependence of $\sigma_n^{-1} d\sigma_n/dy_i$ in the second term (this guess is justified by the analysis of sect. 4.3).

[The fully inclusive correlation function in this "model" is

$$C(y_1, y_2) = (k_0 - 1) \left(\frac{1}{\sigma} \frac{d\sigma}{dy} \right)_{y=0} G(y_1 - y_2) + \left(\frac{1}{\sigma} \frac{d\sigma}{dy_1} \right) \left(\frac{1}{\sigma} \frac{d\sigma}{dy_2} \right) \frac{k_0^2 F_2}{\langle n \rangle^2} \quad (4.5)$$

The last term vanishes if the cluster production multiplicity distribution is Poisson ($F_2 \equiv 0$). More generally, it will be negative ($F_2 < 0$), owing to energy-momentum conservation, even in an independent cluster model.

Eq. (4.5) is obtained after simple algebra upon summing eqs. (4.1) and (4.2) over n and using eq. (2.30). It is, of course, valid only for the "non-diffractive" component of the fully inclusive correlation function.]

The structure of eq. (4.4) is that of a positive term, which is invariant with respect to translations in rapidity [dependence only on $(y_2 - y_1)$], riding upon a negative "background". The positive (Gaussian) term expresses the correlation owing to the existence of clusters. It is suggestive therefore, that one attempt to fit semi-inclusive data to an expression of the form given in eq. (4.4), that is, to a sum of two terms:

$$C_n^{\text{Exp}}(y_1, y_2) = A \exp \left[- \frac{(y_1 - y_2)^2}{4\delta_{\text{exp}}^2} \right] - B \left(\frac{1}{\sigma_n} \frac{d\sigma_n}{dy_1} \right) \left(\frac{1}{\sigma_n} \frac{d\sigma_n}{dy_2} \right) \quad (4.6)$$

According to the model discussed here, one should find that:

- (a) "Correlation length" $2\delta_{\text{exp}}$ is independent of n and s , with $\delta_{\text{exp}} \approx 0.6$ to 0.9 . This length is the distance in $\Delta y = (y_1 - y_2)$ over which the correlation function falls to $1/e$ of its maximum.
- (b) The ratio $A / \left(\frac{1}{\sigma_n} \frac{d\sigma_n}{dy} \right)_{y=0}$ is independent of n and s , provided that the mean number of particles per cluster k_0 is so independent,

as would seem reasonable. Thus, this ratio gives a direct measure of $(k_0 - 1)$ as a function of n .

(c) Coefficient B is equal to (k_0/n) , independent of s . Because $\frac{1}{\sigma_n} \frac{d\sigma_n}{dy} \approx \frac{n}{Y}$, the following additional remark may be added:

$$(d) \quad C_n(0,0) \approx \frac{n}{\log s} \left[\frac{(k_0 - 1)}{2\delta\sqrt{\pi}} - \frac{k_0}{\log s} \right] \quad (4.7)$$

Re-expressed in terms of the popular ratio

$$R_n(y_1, y_2) = C_n \frac{1}{\sigma_n^2} \frac{d\sigma_n}{dy_1} \frac{d\sigma_n}{dy_2}$$

statement (d) becomes

$$R_n(0,0) \approx \frac{\log s}{n} \left[\frac{(k_0 - 1)}{2\delta\sqrt{\pi}} - \frac{k_0}{\log s} \right]. \quad (4.8)$$

Note that $R_n(0,0)$ falls off as n^{-1} and grows as $\log s$. These n and s dependences of $R_n(0,0)$ are in respectable agreement with preliminary ISR results [8] (at which energies $R_n(0,0)$ is positive).

In the simple model discussed here, the linear growth of $C_n(0,0)$ with n appears automatically. However, this prediction is by no means true for all choices of $p(k)$. Thus, as detailed in sect. 4.2, a Poisson form for $p(k)$ gives quite different predictions. Moreover, as discussed in sect. 4.3, kinematic effects and adoption of a more realistic expression for $\sigma_n^{-1} d\sigma_n/dy$ result in a decrease of $n^{-1} C_n(0,0)$ versus n , over the full range of n , even if $p(k) = \delta(k - k_0)$ is retained.

4.2 Broad Intrinsic Cluster Multiplicity Distribution

The second case treated explicitly is that for which $p(k)$ is a Poisson distribution with average $z = \langle k \rangle$, and, again, $\rho_N^{(1)}(y_c) = N/Y$ [c.f. subsection 2.2.1 and eqs. (3.20) and (3.26)]. By contrast to $p(k) = \delta(k - k_0)$, this Poisson example is chosen as representative of a "broad" internal cluster multiplicity distribution.

$$\begin{aligned} \frac{1}{\sigma_n} \frac{d\sigma_n}{dy} &= \frac{1}{Y Q_n} \sum_N N P_N \sum_k \frac{k e^{-Nz} (N-1)^{n-k} z^n}{k! (n-k)!} \\ &= \frac{1}{Y Q_n} \sum_N \frac{N P_N e^{-Nz} z^n}{(n-1)!} \\ &= \frac{n}{Y} \end{aligned} \quad (4.9)$$

$$\begin{aligned} \frac{1}{\sigma_n} \frac{d^2\sigma_n}{dy_1 dy_2} &= G(y_1 - y_2) \frac{1}{Y Q_n} \sum_N N P_N \sum_k \frac{k(k-1) e^{-Nz} (N-1)^{n-k} z^n}{k! (n-k)!} \\ &\quad + \frac{1}{Y^2 Q_n} \sum_N N(N-1) P_N \sum_k \sum_m \frac{km e^{-Nz} z^n (N-2)^{n-k-m}}{k! m! (n-k-m)!} \end{aligned} \quad (4.10)$$

The Gaussian function $G(y_1 - y_2)$ is given in eq. (3.10); P_N is the probability that N clusters are produced.

After modest algebraic simplifications, eq. (4.10) can be reduced to

$$\frac{1}{\sigma_n} \frac{d^2\sigma_n}{dy_1 dy_2} = \frac{(n-1)\langle k \rangle}{Y} \left(\frac{\sigma_{n-1}}{\sigma_n} \right) G(y_1 - y_2) + \frac{n(n-1)}{Y^2} - \frac{(n-1)\langle k \rangle}{Y^2} \left(\frac{\sigma_{n-1}}{\sigma_n} \right). \quad (4.11)$$

Thus, the semi-inclusive correlation function takes the form

$$\begin{aligned} C_n(y_1, y_2) &= \langle k \rangle \left(\frac{\sigma_{n-1}}{\sigma_n} \right) \left(\frac{n-1}{n} \right) \left(\frac{1}{\sigma_n} \frac{d\sigma_n}{dy} \right)_o G(y_1 - y_2) \\ &\quad - \frac{1}{n} \left[1 + \frac{(n-1)}{n} \frac{\sigma_{n-1}}{\sigma_n} \langle k \rangle \right] \left(\frac{1}{\sigma_n} \frac{d\sigma_n}{dy_1} \right) \left(\frac{1}{\sigma_n} \frac{d\sigma_n}{dy_2} \right) \end{aligned} \quad (4.12)$$

All reference to P_N is eliminated in these expressions; instead, the observable partial cross sections σ_n appear as explicit factors.

[The fully-inclusive correlation function is

$$C(y_1, y_2) = \langle k \rangle \left(\frac{1}{\sigma} \frac{d\sigma}{dy} \right)_0 G(y_1 - y_2) + \left(\frac{1}{\sigma} \frac{d\sigma}{dy_1} \right) \left(\frac{1}{\sigma} \frac{d\sigma}{dy_2} \right) \frac{F_2}{\langle N \rangle^2} . \quad (4.13)$$

The same remarks apply here as were made immediately after eq. (4.5).]

The structure of eq. (4.12) is again that of a positive term, which is invariant with respect to translations in rapidity (dependence only on $|y_2 - y_1|$), riding upon a negative "background". The positive (Gaussian) term expresses the correlation owing to the existence of clusters. If one therefore attempts again to fit semi-inclusive data to an expression of the form given by eq. (4.6), one should find that

- (a) "Correlation length" $2\delta_{\text{exp}}$ is independent of n and s , with $\delta_{\text{exp}} \approx 0.6$ to 0.9 , as before.
- (b) The ratio $A / \left(\frac{1}{\sigma_n} \frac{d\sigma_n}{dy} \right)_{y=0}$ is no longer independent of n and s . Indeed, this ratio in general depends strongly on both n and s . As an example, we may choose $n \approx \langle n \rangle$ and fit a Poisson distribution to σ_n locally. Then

$$(n-1) \sigma_{n-1} / n \sigma_n \approx (n-1) / \langle n \rangle .$$

Expanding this expression about $n = \langle n \rangle$, one finds

$$A / \left(\frac{1}{\sigma_n} \frac{d\sigma_n}{dy} \right)_{y=0} \approx \langle k \rangle \left[1 + \frac{(\Delta n - 1)}{\langle n \rangle} \right]$$

In the neighborhood of $n = \langle n \rangle$, the ratio

$$A / \left(\frac{1}{\sigma_n} \frac{d\sigma_n}{dy} \right)_{y=0}$$

thus grows linearly with n , but its derivative decreases as $\langle n \rangle^{-1}$, that is, as $(\log s)^{-1}$. Deviations from the constant prediction of our previous model may not be easy to observe at very high energy, in the relatively narrow range of relevant n values $(\frac{1}{2} \langle n \rangle < n < \sim 2 \langle n \rangle)$.

(c) To further illustrate the contrast between the simple situation $p(k) = \delta(k-k_0)$ and the Poisson choice for $p(k)$, we note that with the Poisson choice, near $n = \langle n \rangle$,

$$C_n(O,O) \propto n^2, \quad (4.14)$$

as opposed to the previous linear growth. Thus,

$$C_n(O,O) = \frac{n}{\log s} \left\{ \frac{\langle k \rangle (n-1)}{2\delta \sqrt{\pi} n} \frac{\sigma_{n-1}}{\sigma_n} - \frac{1}{\log s} \left[1 + \frac{(n-1)}{n} \frac{\sigma_{n-1}}{\sigma_n} \langle k \rangle \right] \right\}. \quad (4.15)$$

$$\approx \frac{n}{\log s} \left\{ \frac{\langle k \rangle (n-1)}{2\delta \sqrt{\pi} \langle n \rangle} - \frac{1}{\log s} \left[1 + \frac{(n-1) \langle k \rangle}{\langle n \rangle} \right] \right\} \quad (4.16)$$

For the ratio $R_n(O,O)$, one finds

$$R_n(O,O) = \frac{\log s}{n} \left[\frac{\langle k \rangle (n-1)}{2\delta \sqrt{\pi} \langle n \rangle} \right] - \frac{1}{n} \left[1 + \frac{\langle k \rangle (n-1)}{\langle n \rangle} \right]. \quad (4.17)$$

In fig. 4, numerical evaluations of eqs. (4.7) and (4.16) are compared. The parameters used are $(k_0 - 1) = \langle k \rangle = 2.6$, $\langle n \rangle = 12$, and $\delta = 0.7$. The choice of $\langle k \rangle = (k_0 - 1)$ imposes equal values in the two models for the fully inclusive correlation function $C(O,O)$.

The contrast in n dependences of $C_n(O,O)$ is understandable physically, at least in a qualitative sense. Imagine that clusters have both an intrinsic multiplicity distribution, which is essentially unobservable, and an effective average multiplicity distribution, which is seen when they contribute to an n hadron final state. These intrinsic and effective spectra are sketched in fig. 5 for the case in which the intrinsic distribution is very broad. If the overall final state multiplicity n is very small, only small k values from each cluster are admissible, and the effective width (dispersion) of the cluster is small. By contrast, if n is large, one may sample k values from the entire $p(k)$, and the effective cluster dispersion will be large. Therefore, if the basic clusters have a very broad $p(k)$, a large n variation of the correlation is inevitable. For very narrow clusters, no such n dependence is possible; one either

samples the cluster or not. The zero width case treated in sect. 4.1 gives the slowest possible rate of growth with n of

$$A \left/ \left(\frac{1}{\sigma_n} \frac{d\sigma_n}{dy} \right)_{y \approx 0} \right. .$$

4.3 "Realistic" Single Particle Spectrum

In sect. 4.1 and 4.2 I focused on the n dependence of $C_n(y_1, y_2)$, as it relates to $p(k)$, the intrinsic cluster multiplicity distribution. In both examples treated, the extreme asymptotic assumption $\rho_N^{(1)} = N/Y$ for the cluster density led to a simple linear growth with n of the single particle y spectrum:

$$\frac{1}{\sigma_n} \frac{d\sigma_n}{dy} = \frac{n}{Y} . \quad (4.18)$$

This is a reasonable if crude approximation to the n and s dependences of $d\sigma_n/dy$ near $y = 0$ [8-10], but it is clearly inadequate outside the central region. Moreover, C_n is computed as the (small) difference of two (large) terms [eq. (2.46)]. The n dependence of $\sigma_n^{-1} d\sigma_n/dy$ enters linearly in the first of these terms, but quadratically in the second. Thus, a systematic deviation from linearity of this n dependence could have pronounced effects on the predicted n dependence of C_n .

In this subsection, I report one investigation of the extent to which (experimental) deviations from eq. (4.18) affect our conclusions. The consequences for C_n are non trivial, but the corrections enter in such a way that the suggested method of data analysis based on fits to eq. (4.6), discussed in sect. 4.1, remains appropriate.

A full treatment of the present issue might be properly carried out with a Monte Carlo simulation of events, in which energy and momentum are conserved properly event-by-event, and in which transverse momentum spectra and leading particle effects (diffraction, etc.) are reproduced [1]. Fortunately, an analytic approach is also possible. I adopt the more general form for the single cluster density, $\rho_N^{(1)}(y_c) = N g_N(Y, y_c)$ [cf. eq. (3.23)], but I retain $p(k) = \delta(k - k_0)$. Thus,

$$\frac{1}{\sigma_n} \frac{d\sigma_n}{dy} = n H_n^{(1)}(Y, Y) = n \int dy_c g_N(Y, Y_c) D^{(1)}(Y, Y_c) \quad (4.19)$$

and

$$\begin{aligned} \frac{1}{\sigma_n} \frac{d^2\sigma_n}{dy_1 dy_2} &= n (k_o - 1) H_n^{(2)}(Y, Y_1 + Y_2) \cdot G(Y_1 - Y_2) \\ &+ n(n - k_o) H_n^{(1)}(Y, Y_1) H_n^{(1)}(Y, Y_2) \quad (4.20) \end{aligned}$$

The correlation function becomes

$$\begin{aligned} C_n(Y_1, Y_2) &= n(k_o - 1) H_n^{(2)}(Y, (Y_1 + Y_2)) G(Y_1 - Y_2) \\ &- n k_o H_n^{(1)}(Y, Y_1) H_n^{(1)}(Y, Y_2) \quad (4.21) \end{aligned}$$

function $G(Y_1 - Y_2)$ is the usual Gaussian, eq. (3.10), and

$$H_n^{(2)}(Y_1, (Y_1 + Y_2)) = \frac{1}{\delta\sqrt{\pi}} \int dy_c g_N(Y, Y_c) \exp \left[-\frac{1}{\delta^2} \left(Y_c - \frac{1}{2} (Y_1 + Y_2) \right)^2 \right] \quad (4.22)$$

In eqs. (4.19) and (4.22), $N \cdot k_o = n$, owing to the choice $p(k) = \delta(k - k_o)$. (I assume that $n = Nk_o$ holds for non integer N and n , also). Expressed in the fashion of our previous results

$$\begin{aligned} C_n(Y_1, Y_2) &= \frac{(k_o - 1) H_n^{(2)}(Y, (Y_1 + Y_2))}{H_n^{(1)}(Y, 0)} \left(\frac{1}{\sigma_n} \frac{d\sigma_n}{dy} \right)_o G(Y_1 - Y_2) \\ &- \frac{k_o}{n} \left(\frac{1}{\sigma_n} \frac{d\sigma_n}{dy_1} \right) \left(\frac{1}{\sigma_n} \frac{d\sigma_n}{dy_2} \right) \quad (4.23) \end{aligned}$$

When compared with eq. (4.4), the present result is seen to possess only one additional factor; namely, the ratio $[H_n^{(2)}/H_n^{(1)}]$, which multiplies the Gaussian. This ratio depends on n , $Y = \log s$, and $(Y_1 + Y_2)$.

$$R_n(Y_1, Y_2) = \frac{1}{n} \left[(k_o - 1) \frac{H_n^{(2)}(Y, (Y_1 + Y_2))}{H_n^{(1)}(Y, Y_1) H_n^{(2)}(Y, Y_2)} G(Y_1 - Y_2) - k_o \right] \quad (4.24)$$

The functions $H_n^{(2)}$ and $H_n^{(1)}$ cannot be obtained unless one is given the cluster density functions $g_N(Y, y_c)$. A reasonable phenomenological procedure would seem to be to determine $g_N(Y, y_c)$ from experimental data on $(n\sigma_n)^{-1} d\sigma_n/dy$ by unfolding eq. (4.19). Having thus determined the $g_N(Y, y_c)$, one may insert them into eq. (4.22) and obtain $H_n^{(2)}(Y, (y_1 + y_2))$.

Not having sufficiently precise data on $\sigma_n^{-1} d\sigma_n/dy$ at either NAL or ISR energies, I follow a somewhat less satisfactory procedure. I adopt Gaussian expressions for $g_N(y_c)$,

$$g_N(y_c) = \frac{1}{d_N \sqrt{2\pi}} \exp(-y_c^2/2 d_N^2), \quad (4.25)$$

and use the energy conservation "sum rule" to determine their dispersions d_N .

No claim is made that Gaussian forms are particularly good either theoretically, or as fits to data. However, they are easy to use and serve the limited purpose intended.

Applying the energy conservation sum rule [24] to clusters at fixed cluster multiplicity N , one may write

$$\int_{E_c} g_N(y_c) dy_c = \sqrt{s}, \quad (4.26)$$

where $E_c = \langle M_T \rangle \cosh y_c$ is the energy of a cluster located at y_c and having mean transverse mass $\langle M_T \rangle = \langle [M^2 + P_T^2]^{1/2} \rangle$. If eq. (3.20) is adopted, one obtains (at large Y) the "prediction"

$$\langle M_T \rangle_N = Y/N \quad (4.27a)$$

Alternatively, if $\rho_N = N/(Y - d_N)$, applicable over a narrower range, $|y_c| \leq Y - d_N$, where d_N is some N dependent cutoff, eq. (4.27a) is replaced by

$$\langle M_T \rangle_N = (Y - d_N)/N \quad (4.27b)$$

Both the rapid decrease with N and the $\log s$ growth with s predicted here seem inconsistent with data [14].

Instead, as a specific analytic approximation for shrinking of the extent in y , as N increases, I use the Gaussian forms, eq. (4.25). The energy sum-rule then requires

$$N \langle M_T \rangle_N \exp \left(\frac{1}{2} d_N^2 \right) = \sqrt{s} ,$$

or

$$d_N^2 = 2 \log \left[\frac{\sqrt{s}}{N \langle M_T \rangle_N} \right] . \quad (4.28)$$

For fixed s , if $\langle M_T \rangle_N$ is fairly constant, as would seem suggested by the rough constancy of $\langle p_T \rangle_n$ as a function of n [14], d_N decreases with N , and $N^{-1} \rho_N(0)$ grows. These are desirable properties. If taken too seriously, however, the s dependence of eq. (4.25) is unreasonable. It is difficult to make consistent with scaling the fully inclusive single particle spectrum. Thus,

$$\left. \frac{d\sigma}{dy} \right|_{y=0} \equiv \sum_N \sigma_N \rho_N \Big|_{y=0} \propto \sum_N \frac{N \sigma_N}{\left[\log (\sqrt{s}/N) \right]^{1/2}}$$

rather than the expected $(d\sigma/dy) = B\sigma$.

I restrict therefore my use of the Gaussian forms to an investigation of the n dependence of $C_n(y_1, y_2)$ at fixed s ; I would not use them to study s dependence at fixed n .

The Gaussian forms can be regarded as cluster density distributions corrected grossly for kinematic (i.e. energy conservation) effects at fixed s .

Having chosen $\langle M_T \rangle_N = 2.0$ GeV, I plot d_N vs. N eq. (4.28) in fig. 6, for two values of \sqrt{s} in the ISR range. The choice $\langle M_T \rangle = 2.0$ GeV, is somewhat arbitrary. However, fits to fully inclusive data suggest $\langle k \rangle \approx 4$ total hadrons per cluster [1,2]. Assigning each of these hadrons 0.4 to 0.5 GeV of energy leads to roughly the correct constant, $\langle p_T \rangle_N$.

In fig. 6, the abscissa is labeled by the cluster multiplicity N . This may be converted to hadron multiplicity n of hadrons of some specific type h upon multiplying N by k_h , where k_h is the multiplicity of type h hadrons in one cluster (e.g. for negative hadrons, $k_h \approx 1$). Note that the dispersion d_N is of order 1 to 2.

In fig. 7, the single hadron inclusive density, divided by n , is plotted versus y for three values of N . These curves are obtained from eqs. (4.19), (4.25) and (4.28), with $\delta = 0.7$, $\langle M_T \rangle = 2$ GeV and $\sqrt{s} = 32$ GeV. Systematic shrinkage of the spread in y is evident as N increases. The rise with N of the $y = 0$ value of these curves is shown in fig. 8a. A 50% increase is present from $N = 3$ to $N = 8$, in contrast to the absence of N dependence associated with the extreme asymptotic expression $\rho_N^{(1)} = N/Y$. This is not a small effect. This increase is forced by the action of energy conservation. The 50% figure may be a slight exaggeration^(*), owing to our use of the Gaussian forms [eq. (4.25)] and assumption that $\langle M_T \rangle$ is independent of N . Ignoring these questions of detail, I retain the present expressions in order to illustrate the effects of a more sensible choice of $\rho_N^{(1)}(y_c)$ on $C_n(y_1, y_2)$.

As remarked just after eq. (4.23), the relevant new factor is the ratio

$$H_n^{(2)}(Y, (y_1 + y_2)) / H_n^{(1)}(Y, 0),$$

which multiplies the Gaussian term in the correlation function. In fig. 9, the function $H_n^{(2)}$ is plotted versus $(y_1 + y_2)$ for three choices of N at $\sqrt{s} = 32$ GeV. For $3 \leq N \leq 7$, it will be noted that $H_n^{(2)}$ changes by at most 14% over the range $0 < (y_1 + y_2) < 2$ (again, $\delta = 0.7$ and $\langle M_T \rangle = 2.0$ GeV). This change is similar for different n values. By contrast, the Gaussian term $G(y_1 - y_2)$ drops by a factor of ~ 8 as Δy changes from 0 to 2. ($\Delta y = |y_1 - y_2|$). Thus in the neighborhood of $y_1 = 0, y_2 = 0$, the y dependence

(*) Note, however, that at 205 GeV/c, $(n\sigma_n)^{-1} d\sigma_n/dy$ at $y=0$ changes from 0.20 at $n=1$ to 0.30 at $n=5$, where n stands for multiplicity of negatives. [Table 2, ref. 10].

of the first term in eq. (4.23) can still be approximated well by $G(y_1 - y_2)$, with the effective dispersion being independent of n .

The ratio $H_n^{(2)}/H_n^{(1)}$ at $y_1=y_2=0$ is shown in fig. 8b as a function of N . It changes by less than 10% over the interval $2 \leq N \leq 10$. Consequently, adopting again the expression suggested in eq. (4.6), I find that the important n dependence of the ratio

$$A \left/ \left(\frac{1}{\sigma_n} \frac{d\sigma_n}{dy} \right)_{y=0} \right.$$

reflects the structure of the internal cluster multiplicity distribution $p(k)$, and is little influenced by assumptions about $\rho_N^{(1)}(y_c)$.

The present analysis, combined with that of sect. 4.1 and 4.2, confirms the utility of eq. (4.6) and suggests that semi-inclusive rapidity correlation data in the region $|y_1| < 2$ and $|y_2| < 2$ be fitted to the (more explicit) form

$$C_n^{\text{Exp}}(y_1, y_2) = \frac{A_0}{2\delta_{\text{exp}} \sqrt{\pi}} \left(\frac{1}{\sigma_n} \frac{d\sigma_n}{dy} \right)_0 \exp \left[- \frac{(y_1 - y_2)^2}{4\delta_{\text{exp}}^2} \right] - \frac{1}{n} (1+A_0) \left(\frac{1}{\sigma_n} \frac{d\sigma_n}{dy_1} \right) \left(\frac{1}{\sigma_n} \frac{d\sigma_n}{dy_2} \right) \quad (4.29)$$

This expression applies for $n > \frac{1}{2} \langle n \rangle$.

The relevant new physics results afforded by semi-inclusive data are the n and s dependences of δ_{exp} and A_0 . In the isotropic cluster approach, δ_{exp} is expected to be independent of n and s , with numerical value $\delta_{\text{exp}} = 0.6$ to 0.9 . (*) The n dependence of A_0 reflects directly the structure of the internal cluster multiplicity distribution $p(k)$. If $p(k)$ is very narrow, A_0 should be independent of n and s [$A_0 \approx \langle k-1 \rangle$ as described in sect. 4.1], whereas if $p(k)$ is broad, A_0 should increase considerably with n [$A_0 \approx (n-1) \langle k \rangle / \langle n \rangle$, as illustrated in sect. 4.2]. The present analysis verifies that these conclusions are independent of our assumptions concerning the n and y dependences of $\sigma_n^{-1} d\sigma_n/dy$, which, a priori, could have influenced conclusions substantially.

(*) These numerical values are appropriate for correlations among pions, which comprise the bulk of hadrons in the central region. For heavier particles, δ is smaller (c.f. sect. 3.1).

In preliminary analysis of ISR correlation data along the lines of eq. (4.29), A_0 is found to vary slowly with n , if at all [8]. Thus, narrow distributions $p(k)$ are favoured. The mean number of hadrons per cluster (charged plus neutral) is between 3 and 4.

Although the conclusions of sect. 4.1 and 4.2 regarding the physical content of the positive Gaussian part of $C_n(y_1, y_2)$ are strengthened by the present investigation, the expected n dependence of $C_n(0,0)$ itself is altered considerably.

Whereas $n^{-1} C_n(0,0)$ is predicted by eq. (4.7) to be independent of n , the analysis of this subsection shows that $n^{-1} C_n(0,0)$ should fall with n . This decrease comes about through the subtraction of the two contributions to $C_n(0,0)$ in eq. (4.23). A numerical evolution of results is given in fig. 8c, for $\sqrt{s} = 32$ and 62 GeV. At sufficiently low s , the decrease of $n^{-1} C_n(0,0)$ with n results in a change of sign of $C_n(0,0)$ as n increases. The choice $k_0 = 2.6$ was made in the numerical evaluation of eq. (4.23), in addition to $\langle M_T \rangle = 2.0$ GeV and $\delta = 0.7$. Thus, the $C_n(0,0)$ values presented are for correlations between two (arbitrary) charged hadrons, in a model in which the mean number of all hadrons (charged plus neutral) per cluster is 4.

The precise numerical values given in figs 7, 8 and 9 should not be taken seriously as quantitative predictions, but rather as qualitative trends. A more reliable phenomenological procedure was suggested above, in which data on $\sigma_n^{-1} d\sigma_n/dy$ are introduced directly, obviating use of the hypothesized Gaussian forms, eq. (4.25).

The kinematic sign change of $C_n(0,0)$ shown in fig. 8c at low values of \sqrt{s} may help to explain the (roughly) zero values for $C_n(0,0)$ observed at 205 GeV/c [10] and, as such, aid in reconciling these data with ISR results [8] at higher \sqrt{s} , where the kinematic (or subtraction) effects are weaker.

In any case, it is clear that a less than linear growth of $C_n(0,0)$ by no means rules out independent cluster emission models, contrary to allegations of Arnold and Thomas [12], and of Morel and Plaut [12].

In fig. 10a, the correlation function $n^{-1} C_n(y,0)$ is plotted versus y for three values of N . ($n \approx k_0 N$). In fig. 10b, $n R_n(y,0)$ is presented. Again, these curves are for charged-charged correlations, at $\sqrt{s} = 32$ GeV. For n not too large, the function $C_n(y_1,0)$ is maximum at $y_1 = y_2 = 0$. It falls off most rapidly from this maximum in the direction $y_1 = -y_2$. In this particular direction, the positive Gaussian part falls as $\exp(-y^2/\delta^2)$. For $y_2 = 0$, the decrease from maximum follows the form $\exp(-y_1^2/4\delta^2)$. As $|y|$ becomes large, the second term in takes over, and $C_n(y,0)$ approaches zero from below.

The positive (Gaussian) term in eq. (4.23) is absent if $k_0 = 1$. This might occur for negative-negative correlations, if the mean number of hadrons per (neutral) cluster is three. Although of limited statistics, data on 205 GeV/c pp collisions studied by the ANL-NAL-SUNY collaboration [10] are indeed consistent with little positive component in $C_n(y_1, y_2)$ above the negative second term in eq. (4.23).

In the absence of the positive correlation component, the function $R_n(y_1, y_2)$ given in eq. (4.24) becomes

$$R_n(y_1, y_2) \rightarrow -k_0/n ,$$

independent of y and s . Data on R_n for negative-negative correlations from the 205 GeV/c analysis are reproduced here as fig. 11. Within statistics they are parametrized effectively as

$$R_n \approx -1/n_-, \quad (4.30)$$

supportive of the conclusion that the average number of negative hadrons per cluster cannot be much above 1 [values greater than 1.3 seem clearly excluded]. That $k_0^{(-)} > 1$, however, [or, more accurately, $(\langle k_0^{(-)2} \rangle / \langle k_0^{(-)} \rangle) > 1$] is indicated by the fully inclusive data which show obvious evidence for elongation of contours along the direction $y_1 = y_2$ [6]. Barring peculiar

behaviour of the cross-term [cf. eq. (3.17)] in the fully inclusive correlation function, this elongation requires positive $\langle k^-(k^- - 1) \rangle / \langle k \rangle$.

Before concluding this section, I remark that if there were correlations between clusters at fixed N , then eq. (3.24) would no longer be valid. This would mean that the second term on the right of eq. (4.29) should be altered to something more complicated. The first term in eq. (4.29) would, however, remain unchanged, since it is independent of the two cluster density.

The first term in eq. (4.29), obviously expresses the correlation coming from within clusters, whereas the second (and possible corrections to the second) relates to correlation between clusters. It would be instructive to attempt an analysis of data in terms of this separation of the two effects.

5. REMARKS AND CONCLUSIONS

The main phenomenological conclusions were stated in the Introduction and in sect. 4.3 and need not be repeated. If analyzed according to eq. (4.29), semi-inclusive rapidity correlation data should provide valuable qualitative insight into the structure of the internal cluster multiplicity distribution $p(k)$ in independent cluster emission models. It is the n dependence of A_o in eq. (4.29) which is most relevant, not that of $C_n(0,0)$ or of $R_n(0,0)$. Owing to the nature of approximations one has to make in order to obtain equations simple enough for confrontation with data, it should be clear that one cannot extract precise quantitative information on $p(k)$. Rather, it appears that we must be content with more casual insight. Data seem to favor a "narrow" spectrum $p(k)$, much more narrow than Poisson, to the extent that A_o is found to be independent of n [8].

The manner in which results are presented in sect. 4 may give the mistaken impression that one can determine $\langle k \rangle$ itself from semi-inclusive data. This is not true. The quantity determined is the n dependence of the ratio of cluster averages

$$A_o \equiv \left(\frac{\langle k(k-1) \rangle}{\langle k \rangle} \right)_n .$$

For the two choices of $p(k)$ which I made, this ratio happens to reduce to $\langle k-1 \rangle$ and $\langle k \rangle (n-1) \sigma_{n-1} / n \sigma_n$, respectively. However, results are in general more complicated.

Although I have concentrated on the variation of A_0 with n , it may be noted that our results suggest that measurement of A_0 at $n \approx \langle n \rangle$ gives an independent determination of the unrestricted ratio

$$\frac{\langle k(k-1) \rangle}{\langle k \rangle}$$

This ratio would be measured directly if one were able to measure the fully inclusive correlation function for the non-diffractive component alone. In fully inclusive data, one observes a melange of non-diffractive and diffractive effects, requiring model dependent assumptions for their separation [1,2]. The semi-inclusive method for (approximate) determination of $\langle k(k-1) \rangle / \langle k \rangle$, without intervention of diffractive effects, may serve as a useful consistency check.

The results given in sect. 4 pertain to $n \gtrsim \frac{1}{2} \langle n \rangle$, where estimates suggest that diffractive effects can be neglected. The semi-inclusive correlations for these values of n should allow direct insight into the "pure non-diffractive" mechanism. For $n < \frac{1}{2} \langle n \rangle$ complications arise [18], and statements are dependent on what one believes about the diffractive mechanism. However, one simple statement is that, just as for the fully-inclusive $C(y_1, y_2)$, the Gaussian part of $C_n(y_1, y_2)$ will sit above a long-range positive "background". Thus, fits to eq. (4.29) for $n \gtrsim \frac{1}{2} \langle n \rangle$ will give values of δ_{exp} which should decrease with n to the n independent values taken on for $n \gtrsim \langle n \rangle$.

As a technical remark, one may add that it is in principle not necessary to employ a 4π solid angle detector to carry out the analyses suggested here. It should suffice, for example, to determine multiplicities n in a counter set-up which covers the central region, say, to the extent of 2π .

My use of the word "independent" in the phrase independent cluster production model deserves comment. By independent, I intend the factored

form of eq. (3.24) for $\rho_N^{(2)}(y_{c1}, y_{c2})$. Specifically I do not assume a Poisson form, or any other form, for P_N the probability distribution for producing N clusters. In the results given in sect. 4.1 and 4.2, the P_N 's do not appear. Wherever they are relevant, it was possible to replace them by observable σ_n 's. If the factored form eq. (3.24) is not adopted, then the second term of eq. (4.29) is considerably more complicated. However, the first term of eq. (4.29) would be unaltered. Thus, it is the n dependence of A_0 as it appears in the first term of eq. (4.29) which is most significant.

Broaching the question of their existence, one may wonder whether clusters are observable more directly than through secondary effects such as discussed in this article [13]. On an intuitive level, it may be imagined that in individual events, the rapidity values of charged particles corresponding to one cluster would be grouped together, with a gap in y separating the tracks of one cluster from those of a neighboring cluster. However, this is not the typical case. Using a logarithmic parametrization, one finds that the mean multiplicity of charged hadrons grows in proportion to $(1.5 \text{ to } 2) \log s$ [25]. Taking $\langle k \rangle = 4$ for the number of hadrons per cluster, we conclude that

$$\langle N \rangle \sim (1. \text{ to } 1.5) \log s .$$

This gives an expected mean spacing of $\Delta y \approx 0.7$ to 1. between cluster centers. Since the spread in y of particles from one cluster is of the same order, the rapidity positions of particles from neighboring clusters will be overlapped in typical events. However, rapidity spectra of events in which transverse momenta are required to be "large", and in which tracks are labeled by their azimuthal angles, might reveal clustering patterns.

By the same token, the cross section σ_N for $N = 2$ clusters should be non-negligible at NAL and ISR energies, since it is a cross section which feeds (e.g.) σ_n for $n = 6$ and 8 charged hadrons. Part of $\sigma_{N=2}$ may be roughly energy independent, corresponding to double diffractive excitation. At NAL and ISR energies, the full range of rapidity available is

large enough so that one should be able to observe the gaps in y space between two clusters, if they are present. Thus an analysis of y spectra for individual low multiplicity events should help in establishing at least whether there is an important two-cluster component. Again, selections on p_T and ϕ could be further instructive.

Acknowledgement

During the course of these investigations I have benefited from discussions with L. Foà and A. Menzione.

REFERENCES

- [1] E.L. Berger and G.C. Fox, Phys. Letters 47B (1973) 162;
E.L. Berger, CERN report ref. TH 1737, to be published in proceedings of the 1973 International School of Subnuclear Physics, Erice, Sicily (Ed. by A. Zichichi).
- [2] P. Piriš and S. Pokorski, Phys. Letters 43B (1973) 502 and Lettere al Nuovo Cimento 8 (1973) 141;
A. Bialas, K. Fialkowski and K. Zalewski, Phys. Letters 45B (1973) 337;
F. Hayot and A. Morel, Nuclear Phys. B68 (1974) 323;
W. Schmidt-Parzefall, Phys. Letters B46 (1973) 399;
C. Quigg, and G.H. Thomas, Phys. Rev. D7 (1973) 2752;
S. Pokorski and L. Van Hove, CERN report ref. TH-1772 (1973);
M. Le Bellac, H. Miettinen, and G. Roberts, Phys. Letters B48 (1974) 115;
C.B. Chiu and K.H. Wang, Phys. Rev. D8 (1973) 2929;
J. Ranft & G. Ranft, Phys. Let. B45 (1973) 43 and Nucl. Phys. B53 (1973) 217;
A.W. Chao and C. Quigg, Phys. Rev. D9 (1974) 2016;
A. Bialas, M. Jacob and S. Pokorski, CERN report ref. TH 1815 (1974).
This list is undoubtedly incomplete; any and all omissions are involuntary, unintended and regretted.
- [3] CERN-Hamburg-Vienna ISR Collaboration. H. Dibon et al., Phys. Letters 44B (1973) 313.
- [4] Pisa-Stony Brook ISR Collaboration. S.R. Amendolia et al., Phys. Letters B48 (1974) 359.
- [5] Argonne-NAL-Stony Brook 205 GeV/c pp Collaboration. R. Singer et al., Argonne report ANL/HEP 7368 (1973).
- [6] Rochester-Michigan 102 GeV/c pp Collaboration. C. Bromberg et al., Rochester report, 1974.
- [7] France-Soviet Union 69 GeV/c pp Serpukhov Collaboration. J. Derre et al., Saclay report M9, submitted to Phys. Letters (1974).

REFERENCES (Cont'd)

- [8] Pisa-Stony Brook ISR Collaboration. L. Foà, Aix-en-Provence Conference, J. de Phys. 34 (1973) 317 and 9th Rencontre de Moriond (1974).
- [9] J. Hanlon, R. Panvini and W. Sims, Nucl. Phys. B52 (1973) 96.
- [10] Argonne-NAL-Stony Brook 205 GeV/c pp Collaboration. R. Singer et al., Argonne Report ANL/HEP 7369 (1973).
- [11] E.L. Berger, Phys. Letters 49B (1974) 369.
- [12] Z. Koba and P. Olesen, Nuovo Cimento 11A (1972) 774;
R.J. Yaes, Lett. al Nuovo Cimento 8 (1973) 365;
J. Ranft & G. Ranft, Phys. Letters 49B (1974) 286 and CERN report ref. TH 1 838
F. Hayot and M. Le Bellac, Michigan report UM-HE 74-7 (1974);
L. Caneschi, CERN report ref. TH 1826 (1974);
R.C. Arnold and G.H. Thomas, Argonne report ANL/HEP 7401 (1974);
A. Morel and G. Plaut, CERN report ref. TH 1865 (1974);
R.D. Peccei, Rutherford report RL-74-050-T.83 (1974); and
M.F. Bourdeau and Ph. Salin, Bordeaux report PTB-57 (1974).
- [13] E.L. Berger and A. Krzywicki, Phys. Letters B36 (1971) 380; and
E.L. Berger, G.C. Fox and A. Krzywicki, Phys. Letters B43 (1973) 132.
- [14] R. Singer, Argonne National Laboratory, private communication.
- [15] British-Scandinavian ISR Collaboration, B. Alper et al., Phys. Letters 47B (1973) 75.
- [16] F.T. Dao et al., Phys. Letters 45B (1973) 402; and S. Barish et al., Argonne Report ANL/HEP 7361, submitted to Phys. Rev.
- [17] W. Frazer and D. Snider, Phys. Letters 45B (1973) 136.
- [18] E.L. Berger, CERN report (1974).

REFERENCES (Cont'd)

- [19] D. Amati, S. Fubini and A. Stanghellini, *Nuovo Cimento* 26 (1962) 896;
and L. Bertocchi, S. Fubini and M. Tonin, *Nuovo Cimento* 25 (1962) 625.

- [20] I.M. Dremin, I.I. Royzen, R.B. White, D.S. Chernavsky, *Zh. Exprim. i Teor. Fiz.* 48 (1965) 952 (*Soviet Phys. JETP* 21 (1965) 633);
V.N. Akimov, D.S. Chernavsky, I.M. Dremin and I.I. Royzen, *Nucl. Phys.* B14 (1969) 285.

- [21] C.J. Hamer, *Phys. Rev.* D7 (1973) 2723;
C.J. Hamer and R.F. Peierls, *Phys. Rev.* D8 (1973) 1358; and
W.R. Frazer, R.D. Peccei, S. Pinsky and C.I. Tan, *Phys. Rev.* D7 (1973) 2647.

- [22] A. Bassetto, Aix-en-Provence Conference Review. *J. de Phys.* 34 (1973) 341.

- [23] Consult, for example, C. DeTar. *Phys. Rev.* D3 (1971) 128.

- [24] T.T. Chou and C.N. Yang. *Phys. Rev. Letters* 25 (1970) 1072;
C. DeTar, D.Z. Freedman and G. Veneziano, *Phys. Rev.* D4 (1971) 906.

- [25] E.L. Berger et al., CERN/D.Ph.II/74-9, (to be published in *Nucl. Phys.*).

FIGURE CAPTIONS

- Fig. 1a Diagram illustrating an amplitude in which clusters of hadrons are produced via a multiperipheral-like exchange mechanism. The exchanges are denoted by dashed lines.
- Fig. 1b Single diffractive excitation diagram, in which a single Pomeron link (wavy line) is present.
- Fig. 2 A numerical study of the single hadron cluster decay function $D^{(1)}(y)$. In (a) it is assumed that an isotropic cluster of mass 1.5 GeV decays at rest into four pions via pure phase space. The curve is reasonably well fitted by the Gaussian form $\exp(-y^2/2\delta^2)$ with $\delta \approx 0.7$. In (b), it is assumed that a cluster of mass 2.4 GeV decays isotropically at rest into three pions plus one nucleon. Decay spectra are shown for the pion and for the nucleon; these curves have dispersions $\delta = 0.72$ and 0.36 , respectively.
- Fig. 3 A numerical evaluation of the two hadron decay function $D^{(2)}(y_1, y_2)$. It is assumed that an isotropic cluster of mass 1.5 GeV decays at rest into four pions via pure phase space. Function $D^{(2)}$ is plotted versus y_2^2 for two selections on y_1 . Fitting these curves to the form $\exp(-y_2^2/2\delta^2)$ one obtains $\delta = 0.67$ for the selection $y_1 < 0.5$ and $\delta = 0.8$ for the selection $y_1 > 1.0$.
- Fig. 4 Correlation function $C_n(y_1, y_2)$ at $y_1 = y_2 = 0$ is plotted versus n . The curves are for the two models, discussed in sect. 4.1 and 4.2, in which the intrinsic cluster multiplicity distribution $p(k)$ is Poisson (solid line) and a delta function (dashed-dot line). Parameters are listed just after eq. (4.17) of the text.
- Fig. 5 A sketch of the intrinsic cluster multiplicity distribution $p(k)$ versus k , with dashed and dot-dashed curves showing the effective distribution when the overall final state hadron multiplicity n is small and large, respectively.

FIGURE CAPTIONS (Cont'd)

- Fig. 6 Dispersion of the cluster density functions, eq. (4.25) of the text, determined from the energy conservation sum rule, at $\sqrt{s} = 32$ and 62 GeV, plotted versus cluster multiplicity N .
- Fig. 7 The single hadron inclusive yield at fixed hadron multiplicity n , divided by n , $(n\sigma_n)^{-1} d\sigma_n/dy$, is plotted versus rapidity y at $\sqrt{s} = 32$ GeV for three different values of the cluster multiplicity N . The values of n and N are related by $n = Nk_0$, where k_0 is the (mean) number per cluster of hadrons of some specific type. These curves are obtained from eqs. (4.19), (4.25) and (4.28) of the text.
- Fig. 8 Plotted versus cluster multiplicity N are (a) the value at $y=0$ of $(n\sigma_n)^{-1} d\sigma_n/dy$; (b) the value at $y=0$ of the ratio $H_n^{(2)}/H_n^{(1)}$, where these quantities are defined by eqs. (4.19) and (4.22) of the text; and (c) the value at $y_1 = y_2 = 0$ of the correlation function C_n divided by n , eq. (4.23) of the text. All results are for $\sqrt{s} = 32$ GeV, except in (c) where values for $\sqrt{s} = 62$ GeV are also shown; n denotes final state hadron multiplicity. Specific parameters used to obtain these results are given in the text.
- Fig. 9 Function $H_n(Y, (y_1+y_2))$, eq. (4.22) of the text, is plotted versus $\frac{1}{2}(y_1+y_2)$ at $\sqrt{s} = 32$ GeV for three values of the cluster multiplicity N .
- Fig. 10 Plotted versus rapidity y for three values of cluster multiplicity N , at $\sqrt{s} = 32$ GeV, are (a) $n^{-1} C_n(y,0)$ and (b) $n R_n(y,0)$.
- Fig. 11 The semi-inclusive correlation function ratio for two negative hadrons, $R_n^{--}(y_1, y_2)$, is plotted versus $\Delta y = (y_1 - y_2)$ for y_1 fixed in two selected intervals. Data are from ref. 10, at 205 GeV/c. Index n denotes multiplicity of negatives: (a) $n = 2$; (b) $n = 3$; and (c) $n = 5$.

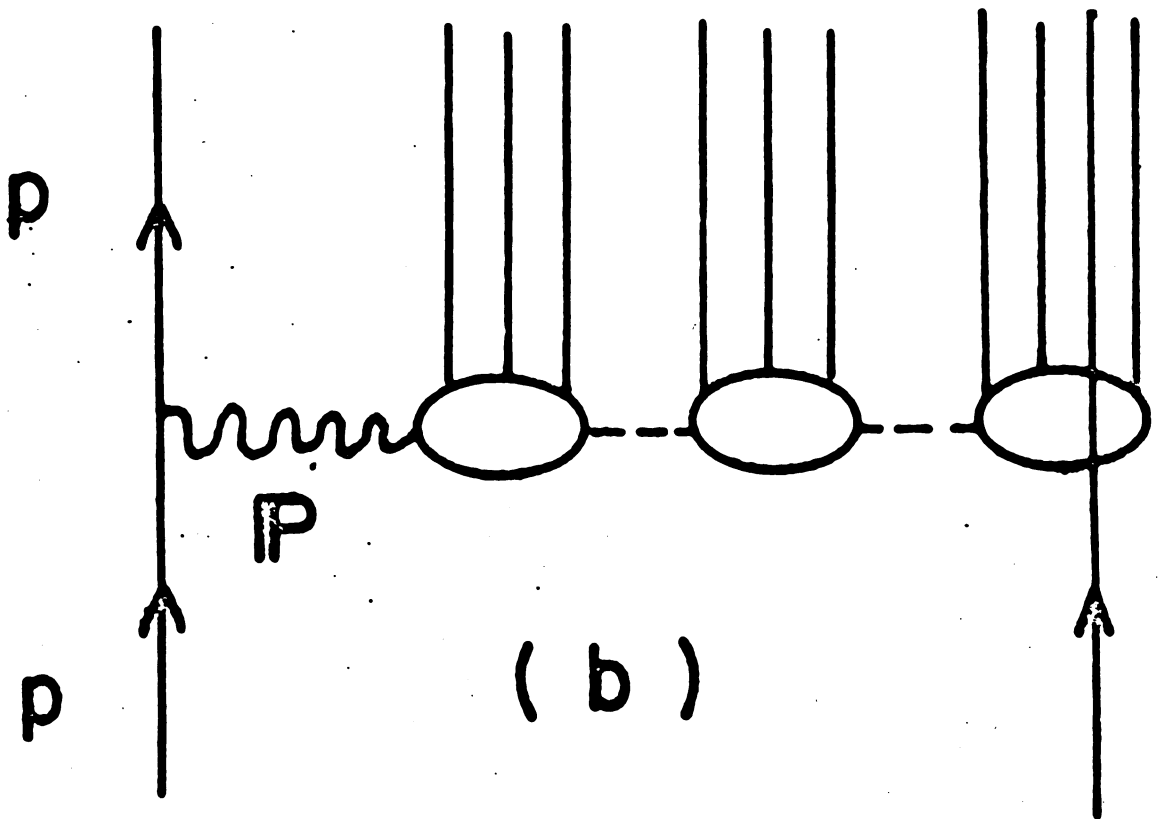
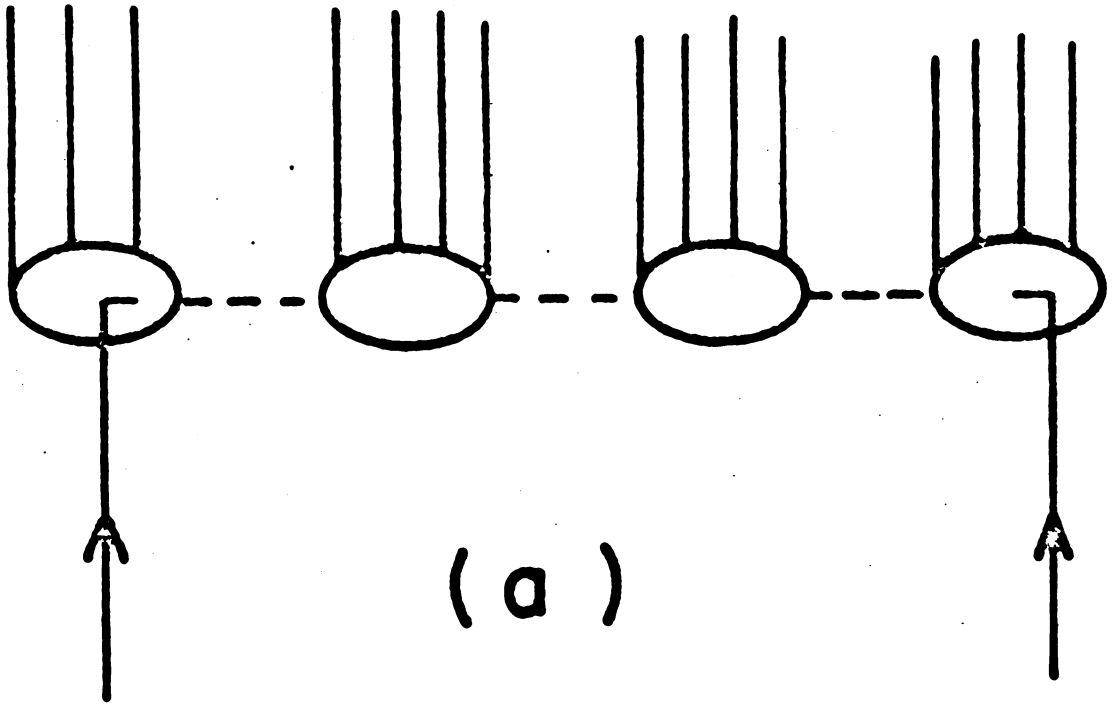


Fig. 1

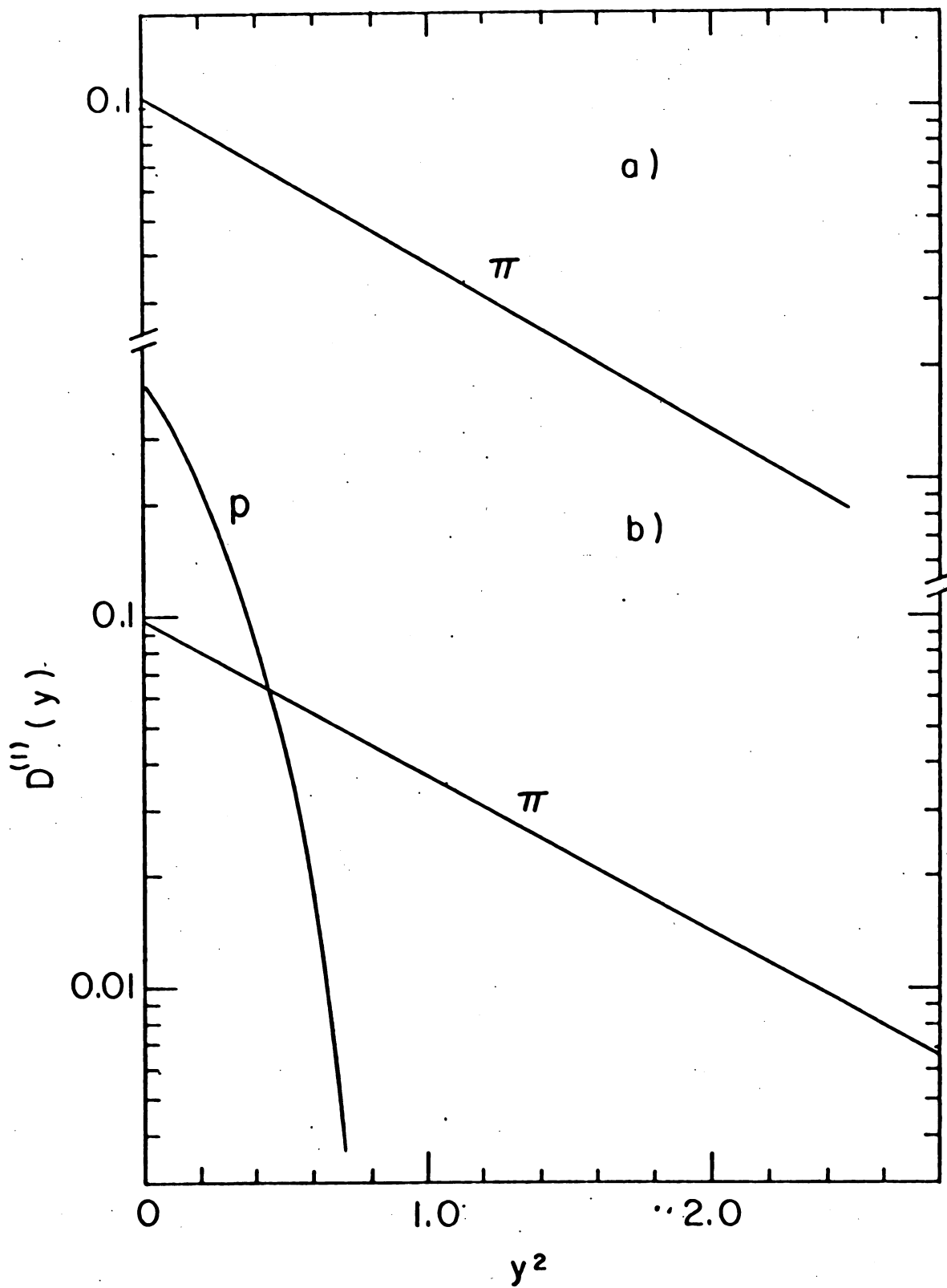
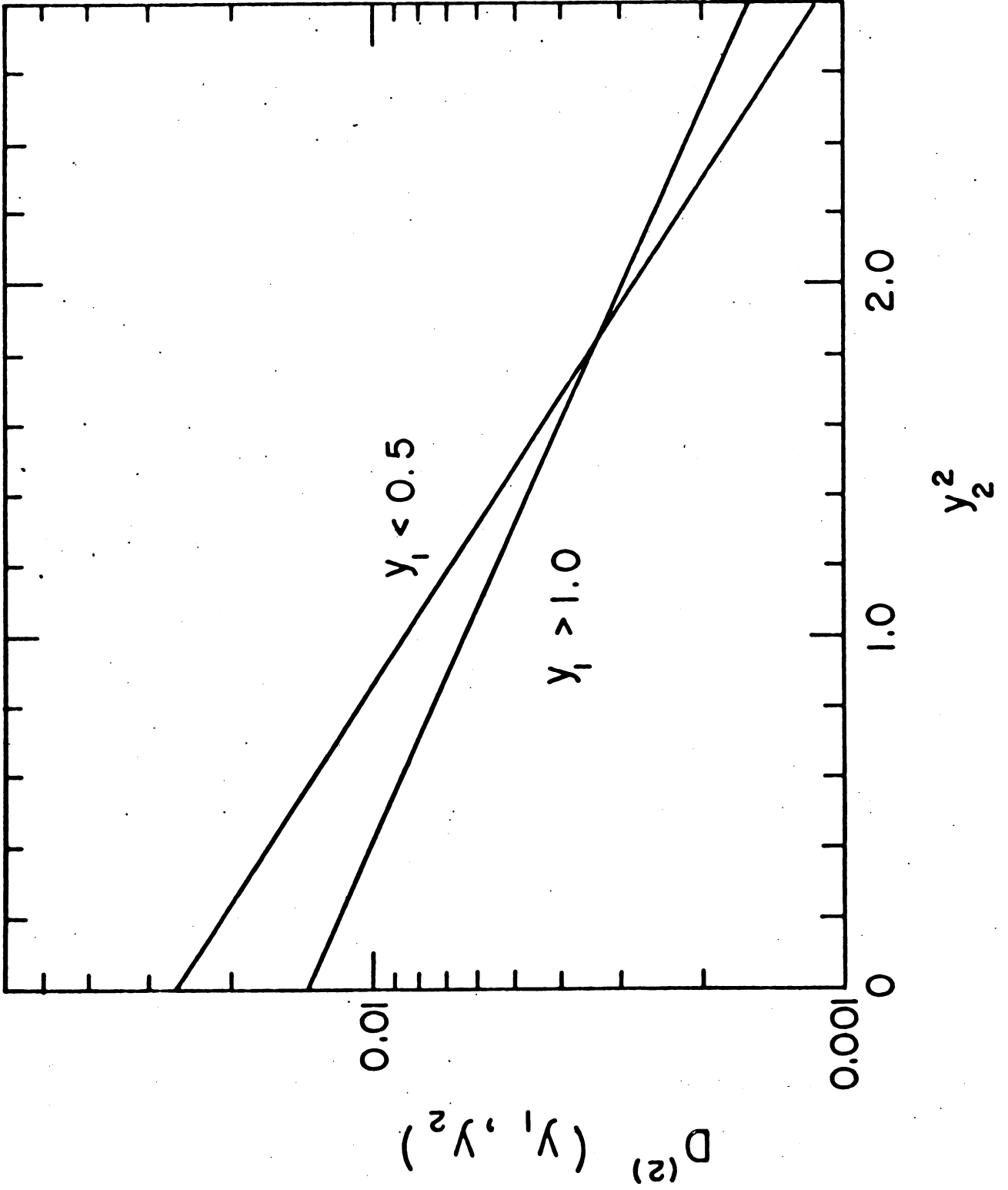


Fig. 2



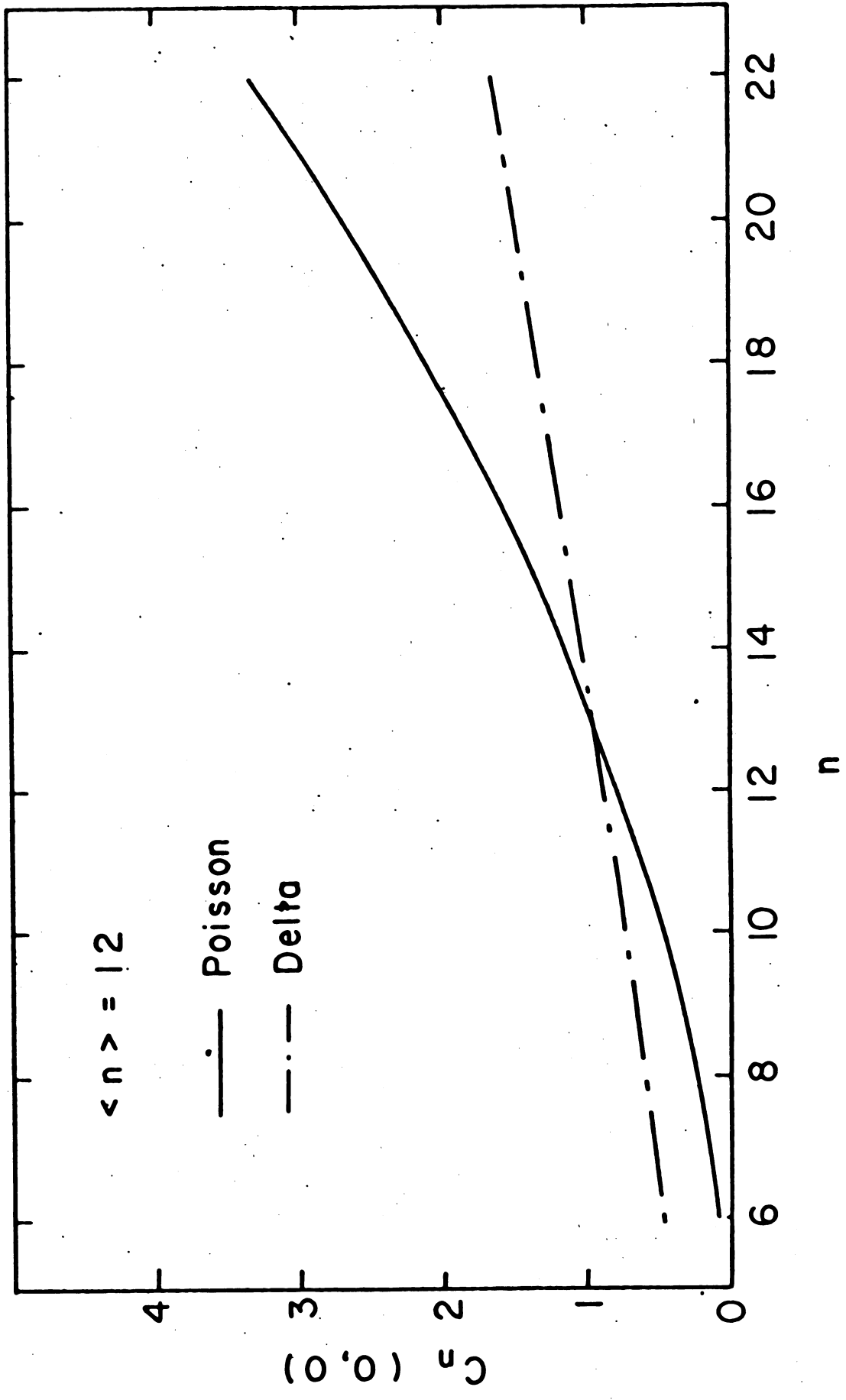


Fig. 4

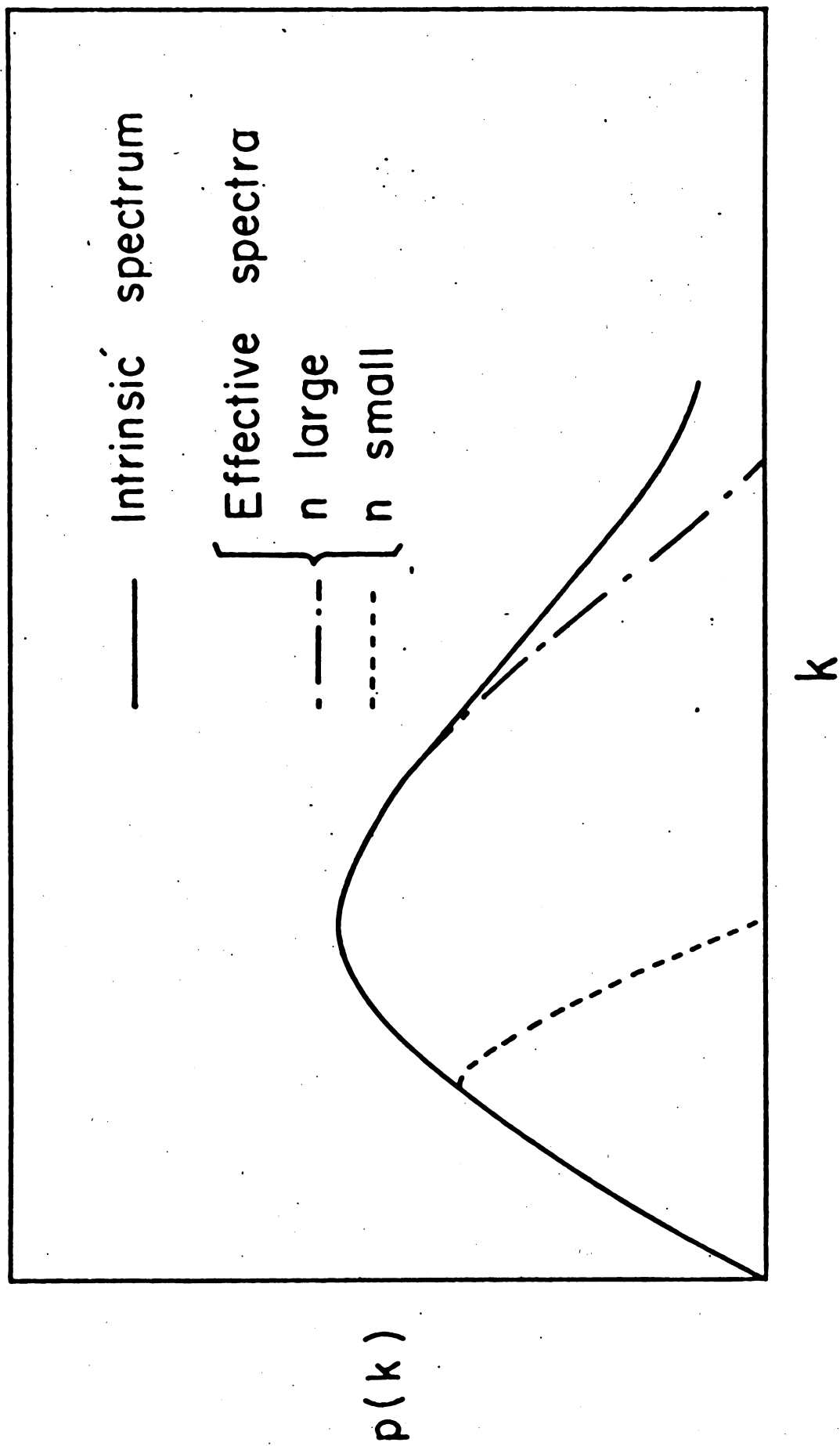


Fig. 5

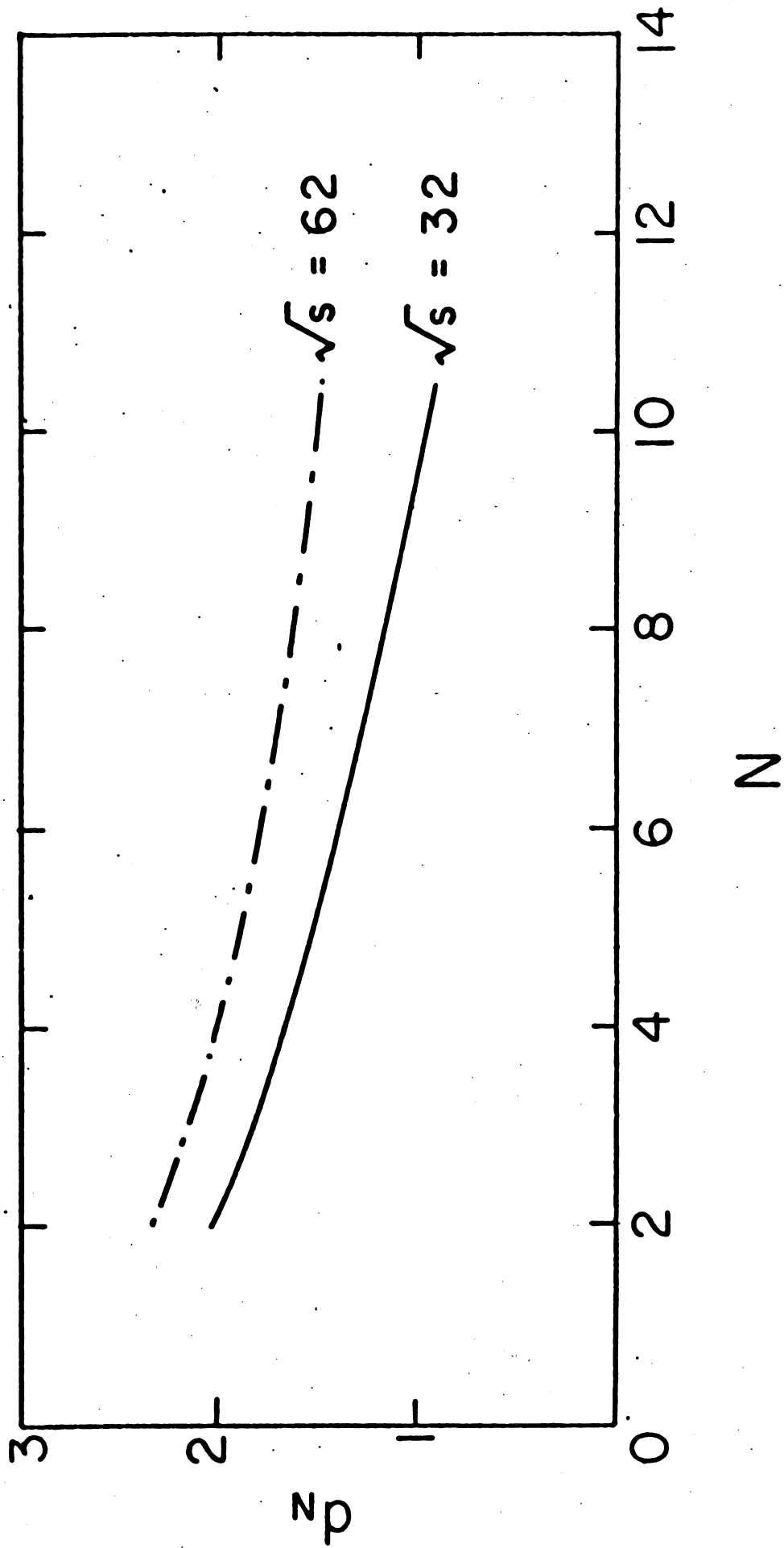


Fig. 6

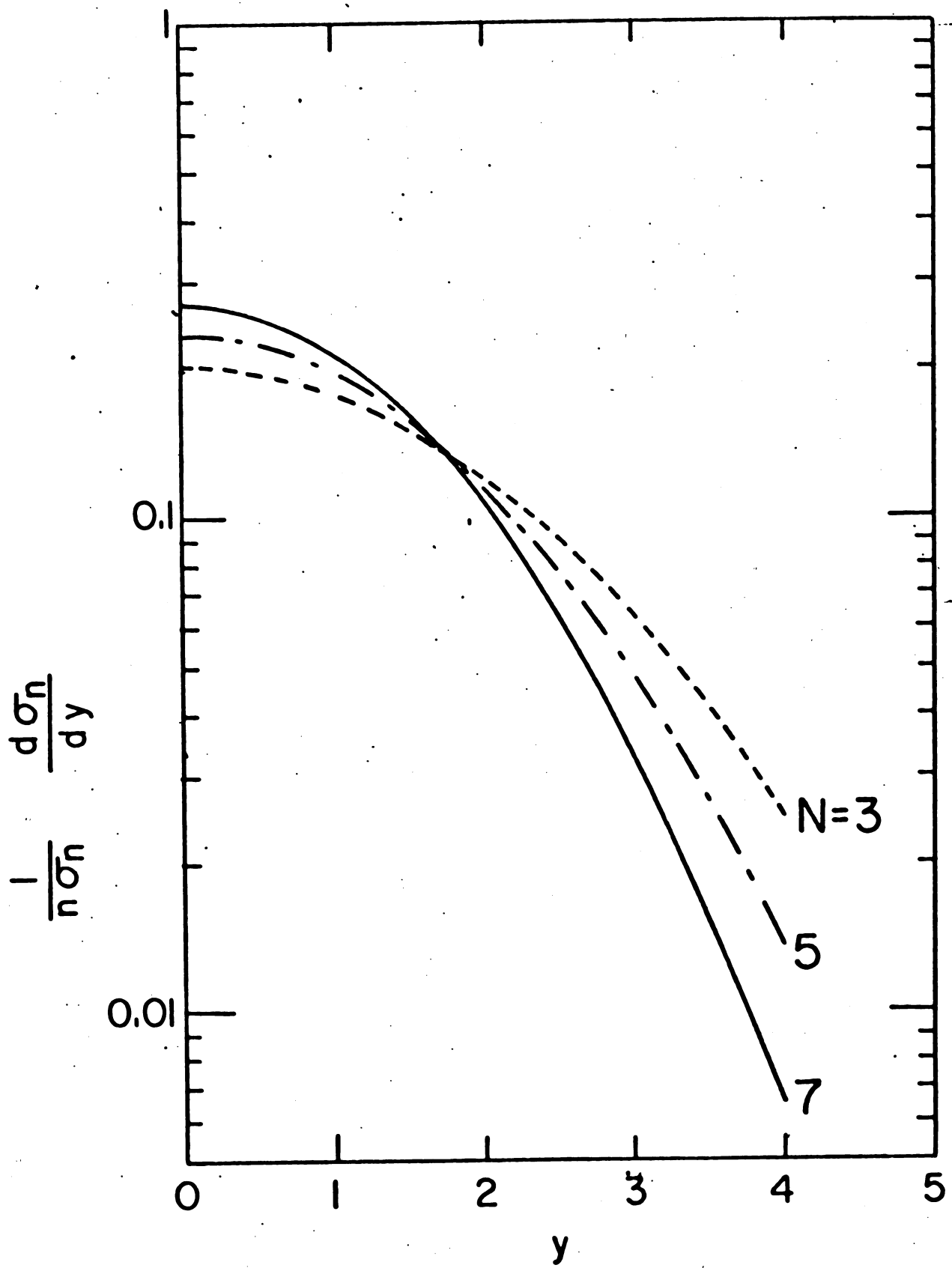


Fig. 7

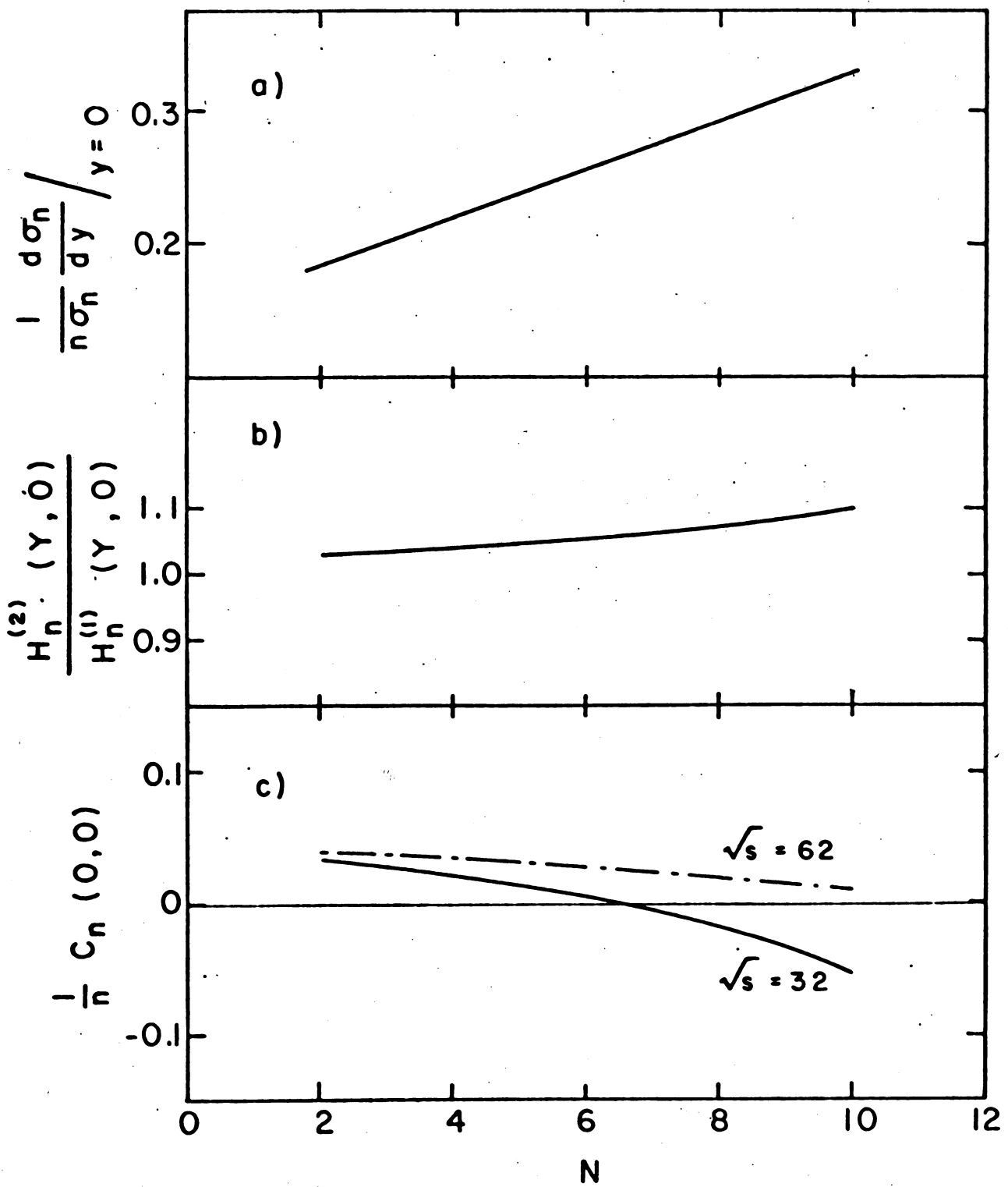


Fig. 8

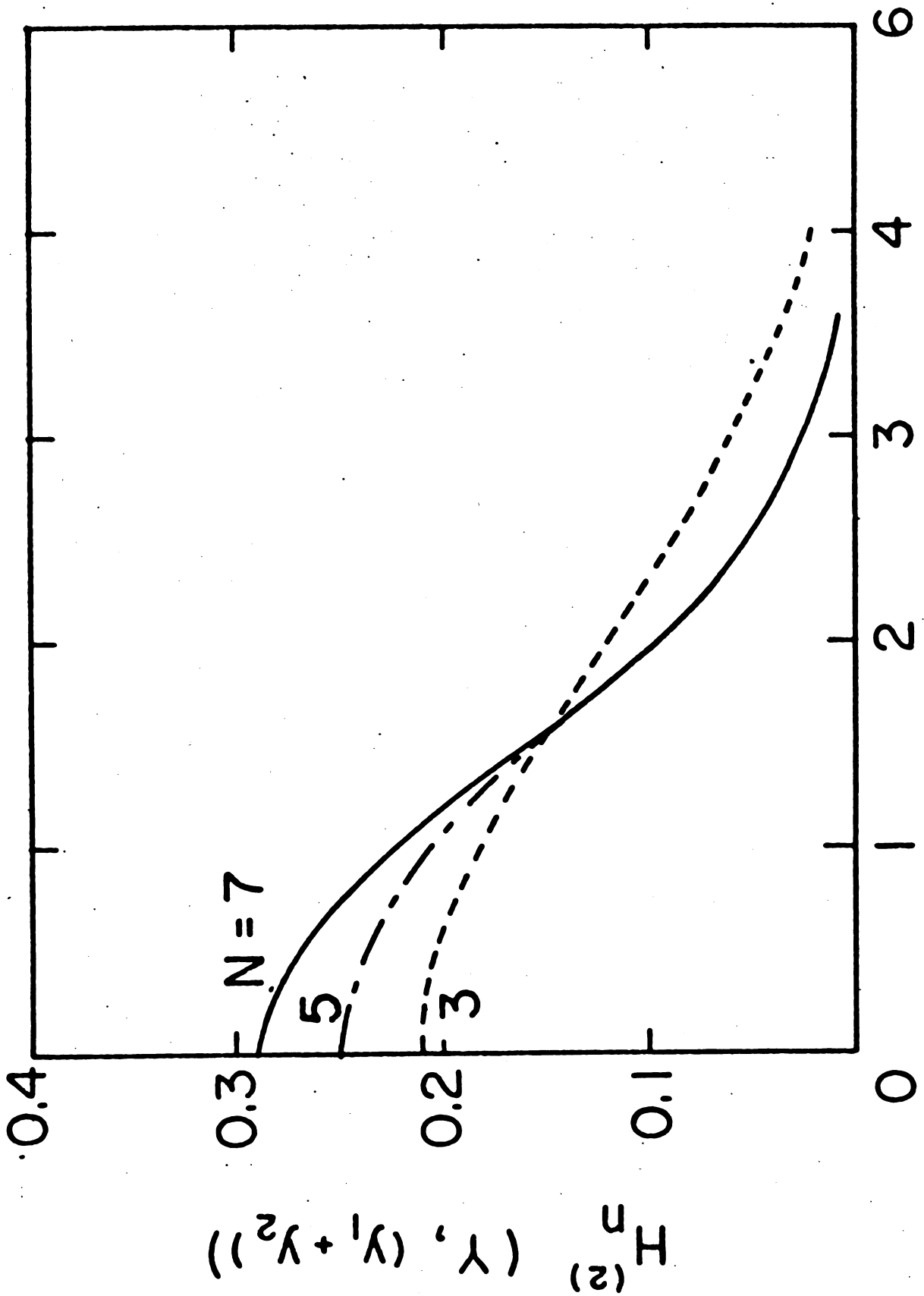


Fig. 9

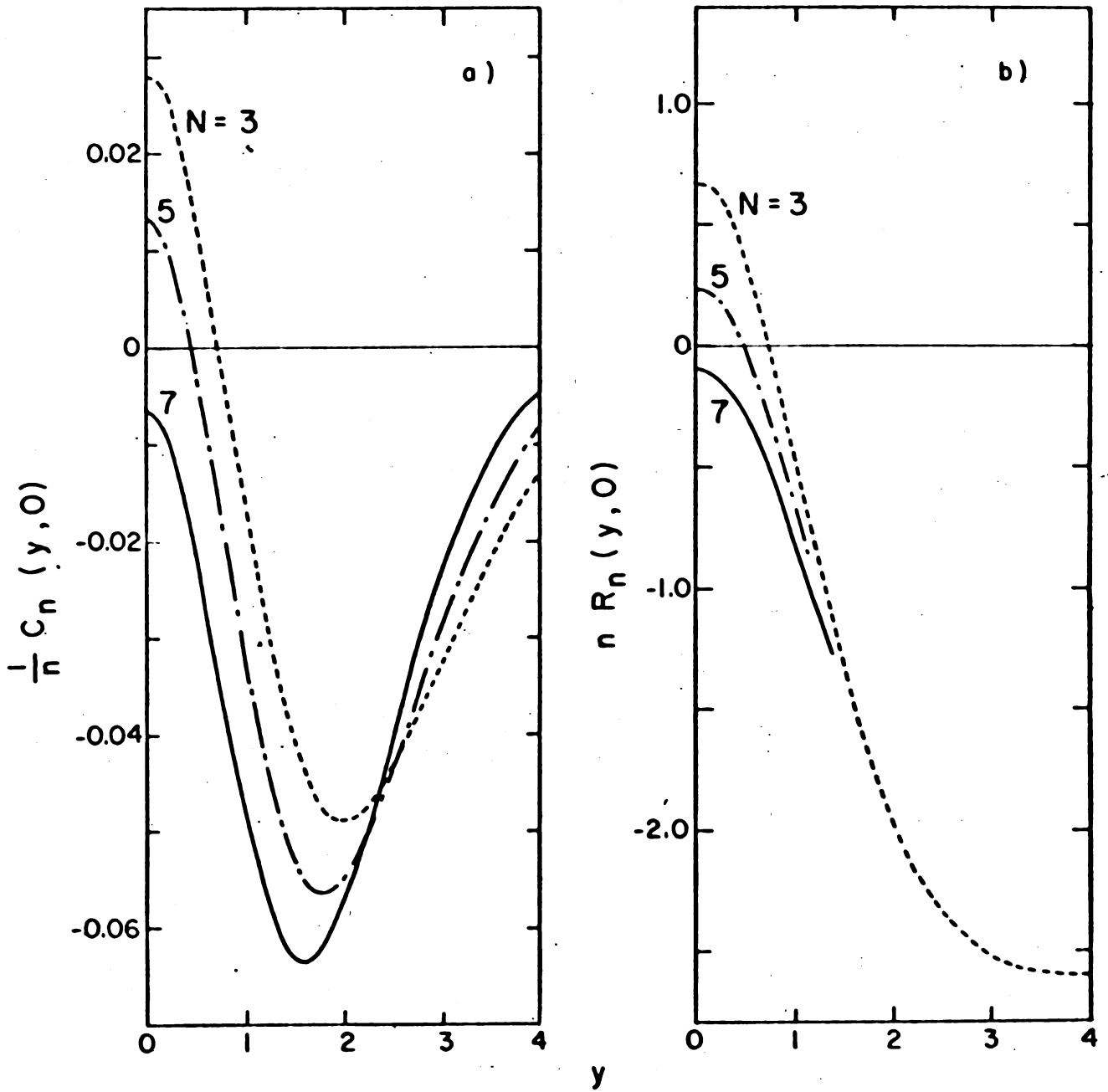


Fig. 10

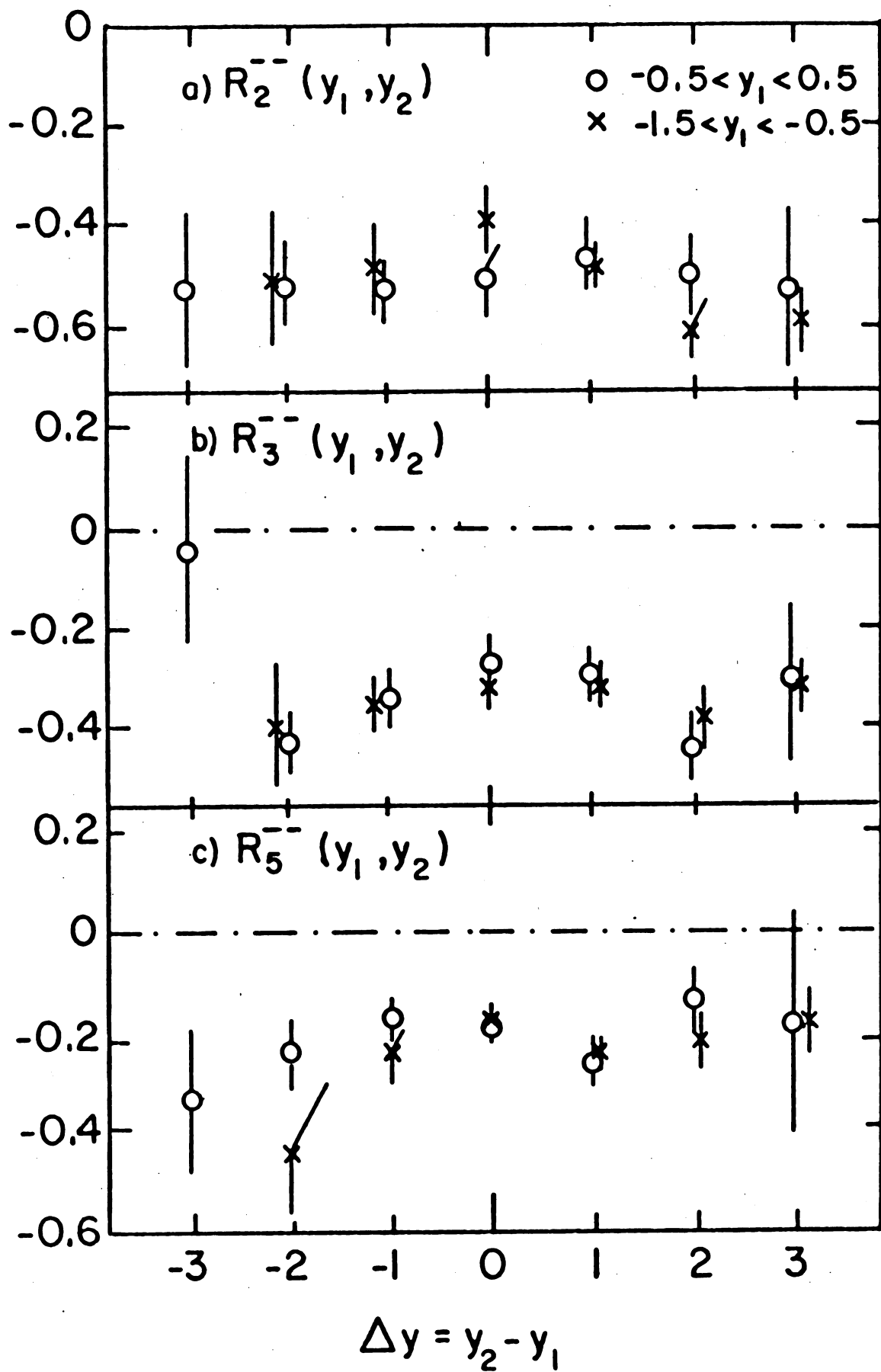


Fig. 11